Anthropocene 49 (2025) 100464

Contents lists available at ScienceDirect

Anthropocene

journal homepage: www.elsevier.com/locate/ancene

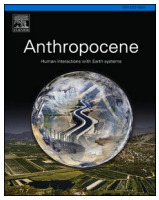

Lead legacy of pre-industrial activities in lake sediments: The case study of the Lake Accesa (Southern Tuscany, Italy)

Francesca Pasquetti [a,*], Giovanni Zanchetta [a], Benoit Caron [b], Julie Noel [b], Riccardo Avanzinelli [c], Boris Vannière [d,e], Marc Desmet [f], Michel Magny [d], Bernd Wagner [g], Luisa Dallai [h], Paolo Fulignati [a], Monica Bini [a], Ilaria Baneschi [i]

[a] Department of Earth Sciences, University of Pisa, Italy
[b] Institut des Sciences de la Terre de Paris, ISTeP UMR 7193, Sorbonne Université, France
[c] Department of Earth Sciences, University of Florence, Italy
[d] MSHE, Chrono-Environment Laboratory, CNRS, Université de Franche-Comté, Besançon, France
[e] Institute of Plant Sciences and Oeschger Center for Climate Change Research, University of Berne, Switzerland
[f] Faculty of Sciences, University of Tours, France
[g] Institute of Geology and Mineralogy, University of Cologne, Germany
[h] Department of Historical Sciences and Cultural Heritage, University of Siena, Italy
[i] Institute of Geosciences and Earth Resources, IGG-CNR, Pisa, Italy

ARTICLE INFO

Keywords:
Trace elements
Pb isotopes
Lake sediments
Mining history
Anthropogenic contamination

ABSTRACT

In recent decades, interest has grown in understanding how pre-industrial activities have contributed to trace metals pollution into the environment at the local and regional scales. Southern Tuscany hosts some of the most important metallogenic provinces in Italy exploited for almost the last three millennia. Studying the history of trace metals pollution in this area offers insights into the temporal and spatial scope of human-environment interactions, evaluates the severity of pollution, and can trace the local natural background values. To explore these aspects, trace metals, major elements, and lead (Pb) isotope ratios were analyzed in an 8000-year sediment records from Lake Accesa, a karst lake located on the southern border of the Colline Metallifere mining district. The findings indicate that Pb in Lake Accesa is mainly related to sulfide polymetallic deposits that surround the lake catchment. The first signal of Pb pollution dates to about 3300 BCE (Before Common Era) during the Copper Age and it is consistent with the archaeological evidence of Southern Tuscany. Additional human-induced Pb pollution signals can be observed in the Bronze Age (~1550 BCE), and a long phase beginning in the Middle Ages (from ~700 CE[Common Era]). Between 1000 and 1700 CE, Pb reached the highest concentrations, corroborating the intensity of mining activity during and after the Medieval period. These findings reveal that pre-industrial activities left a significant legacy of potential toxic elements in the environment, resulting in pollution levels that exceed those related to recent activities associated with the Anthropocene. The Lake Accesa record further indicates that mining of sulfide deposits in the Etruscan period was minimal and even completely negligible during Roman times, probably due to the exploitation of other ore deposits.

1. Introduction

Human activities have strongly altered the natural flux of trace metals into the environment, and it is commonly agreed that the anthropic impact significantly increased after the Industrial Revolution when mining, smelting and industrial processes started to operate on a massive scale. However, in the last decades, geochemical and isotopic studies based on paleoenvironmental records (e.g., ice cores, peat and lake sediments) from different areas worldwide (Cooke et al., 2009; Kamenov et al., 2020; Kern et al., 2021; Lee et al., 2008; Longman et al., 2018; McConnell et al., 2018; Pompeani et al., 2013; Renberg et al., 2000) have shown that human beings have impacted and altered the environment much earlier than the Industrial Revolution. For example, the beginning of agriculture in the Holocene and the application of fire regimes for specific activities produced environmental signatures that can be recognized today in the sedimentary records (e.g., Hawthorne

* Corresponding author.
E-mail address: francesca.pasquetti@phd.unipi.it (F. Pasquetti).

https://doi.org/10.1016/j.ancene.2025.100464
Received 3 November 2023; Received in revised form 29 October 2024; Accepted 17 January 2025
Available online 4 February 2025

and Mitchell, 2016; Vannière et al., 2008). Mining and metallurgical activities certainly released substantial amounts of trace metals into the environment in the pre-industrial period (e.g., Elbaz-Poulichet et al., 2020; Kern et al., 2021; Kylander et al., 2005; Renberg et al., 2000). In the Mediterranean area, mining and metallurgical activities have been so massive and prolonged (e.g., Kassianidou and Knapp, 2005) that their signature can even be identified in Greenland ice-cores (McConnell et al., 2019, 2018 and reference therein). This creates considerable general interest in understanding how, and to what degree, pre-industrial activities have contributed to trace metals pollution into the environment at different scales (e.g., local and regional). The study of trace metals pollution provides insights into temporal and spatial scope of human-environment interactions and allows evaluation of the severity of pollution and the natural background conditions of the selected areas.

The Colline Metallifere district (southern Tuscany, Italy; Fig. 1) is an important metallogenic province in Italy exploited for almost the last three millennia (e.g., Dini, 2003). During this period, ore deposits were mined with varying intensity (e.g., Benvenuti et al., 2014). According to historical and archaeological records, the extraction of mixed sulfides of copper, lead and silver was particularly consistent during the central centuries of the Middle Ages, and their use was linked, among others, to coinage (Chiarantini et al., 2021; Poggi et al., 2023). Although, formally, underground resources remained in the hands of public authority, from the 11th century CE (Common Era) onwards, important seigniorial families held true control of the territorial economical assets. Between the end of the 11th and the 13th century CE, through the so-called "mining castles" (i.e., highly efficient land management and resource exploitation centres), aristocracies developed a strict control over mining areas; mine economy led, at this chronological hight, to the development of distinctive social and economic settlement patterns (Bianchi, 2022; Francovich and Wickham, 1994). From the mid-13th century and throughout the 14th century CE, mining and metallurgical activities were also subject to the progressive expansion of municipal control, which in this territory was associated with the redaction of a remarkable body of written regulations, the *Ordinamenta super arte fossarum rameriae et argenteriae civitatis Massae*, subsequently included in the statute of the town of Massa Marittima (Dallai, 2014). After a long phase of decline, the end of the 19th century CE and the first half of the 20th century CE saw the revival of the large-scale extractive industry. This recent industrial phase pursued until the end of the 1980s, when most of the mines were closed throughout the region. For these reasons, southern Tuscany represents an extremely interesting case-study area to investigate the history of trace metals pollution and get insights into the contributions of industrial and pre-industrial activities over time.

For this purpose, we performed major, trace elements and lead (Pb) isotope analysis in an 8000 year-long lacustrine deposition in southern Tuscany. The sediment cores analyzed in this study were collected from Lake Accesa, a small karstic lake (~0.14 km^2) located about 5 km from the town of Massa Marittima (Fig. 1). The study mainly focused on Pb, which is associated with many polymetallic ores (e.g., Cooke and Bindler, 2015; Kern et al., 2021), tends to be geochemically stable in sedimentary deposits (e.g., Gallon et al., 2004) and has four stable isotopes that can be used to distinguish between anthropogenic and natural geogenic sources (Bindler et al., 2008; Stos-Gale and Gale, 2009). Moreover, Pb has a long residence time in the atmosphere (e.g., Elbaz-Poulichet et al., 2020) which allows supra-regional dispersion. This is why Pb is one of the oldest and most widespread anthropogenic contaminants and it is among the most studied pollutants around the world (Kern et al., 2021; Kylander et al., 2005; Longman et al., 2018; McConnell et al., 2018).

All the elements analysed in this study were combined to answer the following questions: i) What are the prehistoric-historical trends of Pb, and other trace elements associated with sulfides ore deposits, such as copper (Cu) and zinc (Zn)? ii) Are there potential processes affecting their distributions in the sedimentary record? iii) What are the potential sources for these elements? iv) Have pre-industrial activities left a legacy of potential toxic elements in this area?

2. Study area and prehistoric-historical context

Lake Accesa (42°59′17″N, 10°53′44″E) is a water-filled karst sinkhole located in southern Tuscany (central Italy) at 157 m a.s.l., on the southern border of the Colline Metallifere mining district (Fig. 1), which is characterized by widespread hydrothermal mineralization (Dini, 2003). The lake surface measures ca. 0.14 km^2. The catchment area covers ca. 5 km^2 and is delimited by hills culminating at ca. 320 m a.s.l. (Fig. 2 A). The geology of the catchment is characterized by large outcrops of the Triassic limestone "Calcare Cavernoso", which constitute the main aquifer of the area. The catchment also includes Triassic phyllites and Cretacic shales overlaid by Miocene sediments and Quaternary deposits (Fig. 2 A). The lake has a sub-circular shape and reaches a maximum depth of 38.5 m (Fig. 2 B; Tassi et al., 2014). Lake Accesa has no surface tributaries and is mainly fed by a sub-aerial (named

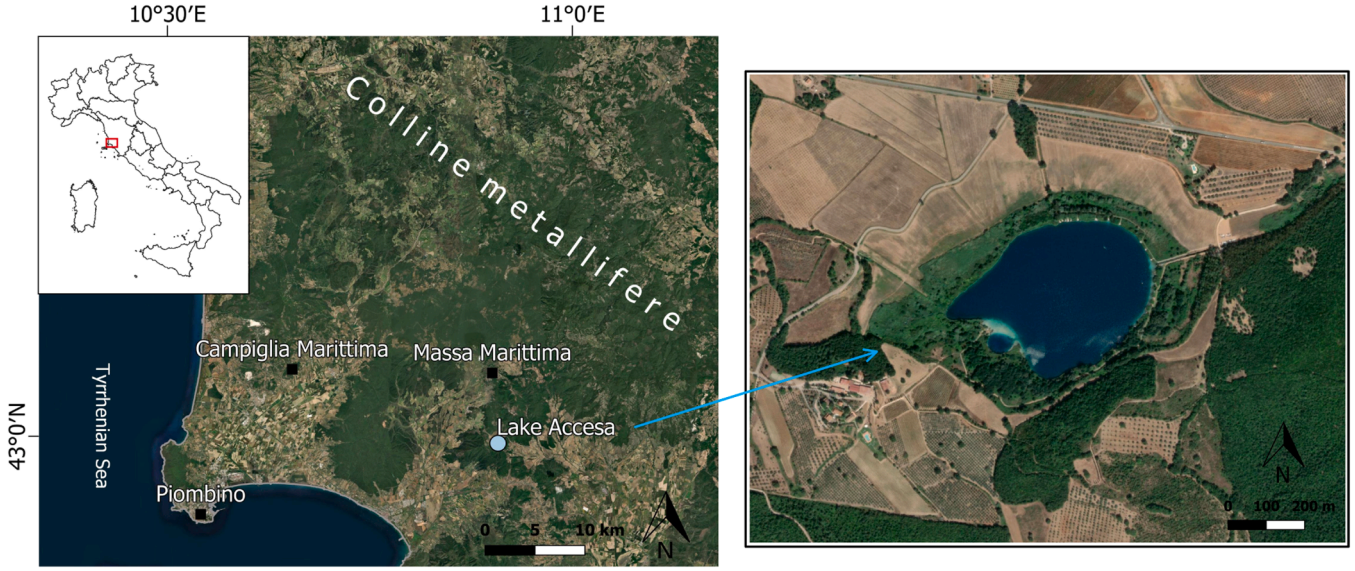

Fig. 1. Localization of Colline Metallifere district and Lake Accesa on the left, and satellite photo of the lake on the right (ESRI World imagery).

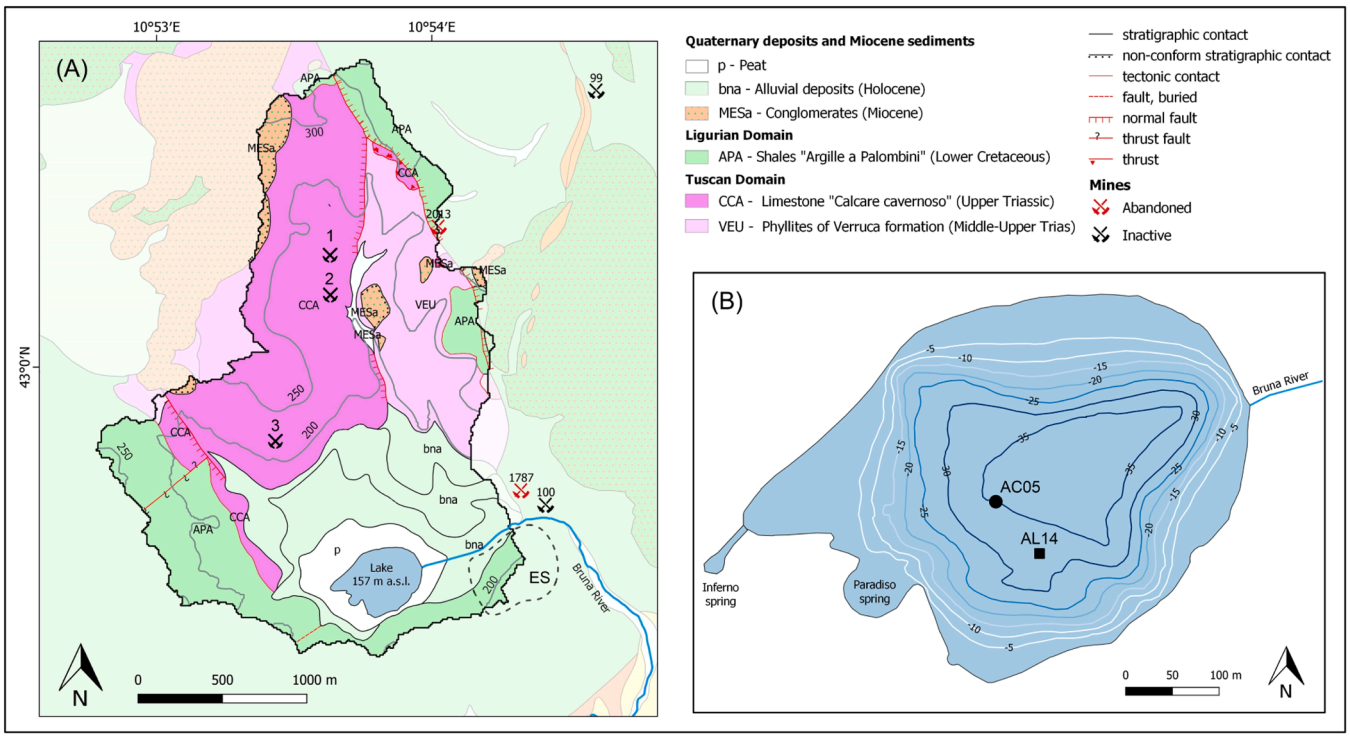

Fig. 2. (A) Geological map of the catchment area of Lake Accesa (Tuscan Geological Database in scale 1:10000 available as shapefile on http://www502.regione.toscana.it/geoscopio). Location and information about mines are downloaded from the Italian database of mines (https://www.isprambiente.gov.it) and from the pre-industrial mining dataset (DSSBC) of the University of Siena: n°99 – Fenice Capanne (metal-sulfur ore deposits); n°100 –La Pesta (metal-sulfur ore deposits); n° 1787 Carpignone (metal-sulfur ore deposits); n° 2013 Allumiere (aluminum ore deposits, alunite); n°1: Poggio Salcerini (metal-sulfur ore deposit); n°2: Val di Strega (metal-sulfur ore deposit); n°3: Infernuccio (metal-sulfur ore deposit). ES: Etruscan site delimited by dashed line (Camporeale, 2002). (B) Bathymetric map of Lake Accesa (isobaths: 5 m; reproduced after Tassi et al. 2014) with location of thermal springs that fed the lake and sediment cores analyzed in this study.

"Inferno") and a sub-aqueous (named "Paradiso") thermal springs (Vannière et al., 2008), which uprise along the fault system of the area (Fig. 2). Therefore, although the surficial drainage basin area is small, the lake collects water from a larger basin. The outlet of the lake is the Bruna River (Fig. 2 B). The water of the lake is characterized by Ca-SO_4 composition and relatively high total dissolved solids (Tassi et al., 2014).

Nowadays, the area around the lake consists mainly of agricultural and wooded land, the latter characterized by mixed evergreen, deciduous forests (e.g., *Quercus ilex*, *Q. pubescens*). In the catchment area and its realm there are several abandoned and inactive mines (Fig. 2 A), which are mainly constituted by sulfide polymetallic Cu-Pb-Zn-(Ag) deposits (Arisi Rota and Vighi, 1971; Tanelli, 1983). Remains of an Etruscan settlement discovered near the lake (Fig. 2 A) suppose that these deposits have been exploited at least since the Etruscan times. According to Camporeale (2017) this settlement lasted about three centuries, from 8th to 6th century BCE (Before Common Era), and the mining vocation is suggested by the discovery of furnaces for the roasting of ore material (Camporeale, 2002). Moreover, minerals from other areas could also have been processed at this site because historical sources report that the water of the Bruna River was used to wash minerals from the island of Elba and from regional and local mines (Rizzotto, 1981). Other artifacts and archaeological remains indicate that the area was occupied by humans continuously during the Hellenistic and Roman period (Camporeale, 2000). Pollen investigations highlighted human-induced changes in vegetation since ca. 8000 cal. BP (Before Present, Present: 1950) with a growing impact from ca. 4500 cal. BP (Drescher-Schneider et al., 2007).

3. Materials and methods

3.1. Sediment cores, age-depth models, and sampling

The main core analyzed in this study (core AC05) was collected in 2005 from a well stratified and undisturbed part of the deep-basin sedimentary infilling of Lake Accesa (Fig. 2 B). The core is about 8 m long and covers the last 11500 cal. BP according to an age-depth model based on 11 Accelerator Mass Spectrometry (AMS) ^{14}C ages from terrestrial plant macrofossils (Vannière et al., 2008). From this core, 35 samples were collected for trace and major elements analysis. Sample intervals were selected to provide a mean resolution of about 80 years for the last 1000 cal. BP and about 300 years until 8000 cal. BP (sampling stopped at ~6 m). Seven of these samples were also analyzed for Pb isotopes and three were investigated under the scanning electron microscopy. For the same core, unpublished XRF (X-Ray Fluorescence) analysis for Pb on discrete samples were also available. For this dataset, data resolution was about 2 cm from the top to a depth of 5 m and about 25 cm below.

Data obtained from the core AC05 was compared with high-resolution XRF scanning data obtained from the core AL14 that was collected from a water depth of 35.1 m at N 42°59.254' and E 010°53.738' ca. 70 m to the southeast of AC05, in 2014 (Fig. 2 B). The correlation of core segments was determined using optical images and lithological data (Fig. S1 of the supplementary material). The total length of AL14 is about 13 m of which the upper 8 m show very similar lithology and physiochemical characteristics (e.g., Ca and total organic carbon (TOC) contents) compared to core AC05 (Fig. S1 of the supplementary material). This made it possible to transfer the AMS radiocarbon dates measured on the core AC05 (Vannière et al., 2008) to the core AL14. The radiocarbon dates were re-calibrated using the updated ^{14}C calibration curve for the Northern Hemisphere (Reimer et al., 2020)

and an age-depth model was calculated using the Bacon software (Blaauw et al., 2018).

3.2. Analytical methods

3.2.1. Core AC05

3.2.1.1. Trace and major elements. All samples were dried at room temperature and then ground to a powder using an agata mortar. Trace (Li, V, Cr, Ni, Cu, Zn, Ga, Rb, Sr, Y, Zr, Nb, Cs, Ba, Hf, Ta, Th, U, La, Ce, Eu, Pb) and major elements (Al, Si, Ca, Mg, Mn, Na, P, Fe, K, Ti) characterization of the 35 samples were performed by Inductively Coupled Plasma Mass Spectrometry (ICP-MS) and Inductively Coupled Plasma Optical Emission Spectroscopy (ICP-OES), respectively, at the ALIPP6 facilities (Sorbonne Université, ISTeP). ICP-MS analyses were carried out using an 8900 Agilent ICP-MS/MS, while ICP-OES analyses were performed using a 5100 SVDV Agilent ICP-OES (Mauran et al., 2022, 2021).

For both types of analyses, 50 mg of homogenized powder were digested in acidic solutions (a mixture of Suprapur® HF (1 ml, 40 % w/w) and HNO_3 (1 ml, 69 % w/w)) inside a Polypropylene DigiTUBE. After complete digestion, the samples were evaporated using DigiPREP (SCP Sciences) hot blocks. Then, 1 ml of H_2O_2 was added to the samples to completely digest organic matter. After complete evaporation, 1 ml of boric acid (H_3BO_3) was used to neutralize eventual excess of HF. When samples were dry, they were diluted with MilliQ HNO_3 2 % v/v. Blank, international and internal standards were digested each time. Several standards with different elemental concentrations (AGV-1, BE-N, BHVO-2, BIR-1, RGM-1, MAG-1) were used for the external calibration and to check the accuracy of the results that is < 7 %, except for a few elements (Table S1 of Supplementary Material). BHVO-2 was also used to detect and correct for any signal drift. For each analyzed element, the measurement was performed in triplicates. The results were averaged and considered acceptable when the RSD is < 10 %. The detection limit (DL) was calculated on data in count per second (CPS) following the equation: $DL = x_{blank} + 3 * SD$, where x_{blank} and SD are the mean and the standard deviation of results obtained from three samples of blank analyzed three times in triplicates. All results higher than DL were corrected for the blank signal (i.e., the mean value for blank in CPS was subtracted from sample results). Results for trace elements are given in ppm (mg/kg) while results for major elements are given in wt%.

Carbonate contents were calculated *via* a gasometric technique that relies on the chemical reaction of carbonates with 10 wt% HCl. The CO_2 released is measured through a sealed cylinder filled with super-saturated potassium chloride (KCl). The carbonate content was calculated after external calibration with known amounts of pure $CaCO_3$. The accuracy is < 7 % while the RSD of each analysis is < 5 %. In this case we considered as <DL values < 5 %. Raw data are listed in Table S2 of the supplementary material.

3.2.1.2. Lead isotopes. Lead isotope ratios ($^{206}Pb/^{204}Pb$, $^{207}Pb/^{204}Pb$ and $^{208}Pb/^{204}Pb$) were measured with a Thermal Ionisation Mass Spectrometer (TIMS) ThermoFinnigan Triton-Ti®.

Seven powdered samples were weighed to obtain approximately 200 ng of lead. Powders were then dissolved by sequential HF–HNO_3–HCl dissolution and purified by extraction chromatography using ultra-pure quality acids and Teflon micro-columns filled with about 100 µl of AG1x8 resin (100–150 µm, Eichrom®), as described in Avanzinelli et al. (2014). Instrumental mass bias was corrected using replicate analyses of NIST SRM 981 standard. A fractionation factor of 0.140 % per mass unit relative to the reference values (Baker et al., 2004) was applied to all Pb isotope ratios. The accuracy was evaluated by replicate measurements of the international standard AGV-1, yielding average values of $^{206}Pb/^{204}Pb$ 18.947 ± 0.006, $^{207}Pb/^{204}Pb$ 15.663 ± 0.007 and $^{208}Pb/^{204}Pb$ 38.576 ± 0.024 (2σ, n = 12), which are within errors of the values reported by Weis et al. (2006). The results are reported in Table S3 of the supplementary material.

3.2.1.3. Electron microscopy. Scanning electron microscopy analyses were performed using a field emission scanning electron microscope (FEI QUANTA 450 ESEM-FEG). The instrument operated at high vacuum (< 6 e^{-4} Pa) and nominal 1 nm electron beam resolution at 20 kV acceleration voltage and was equipped with a Bruker's QUANTAX XFlash Detector 6|10 for microanalyses and X-ray compositional mapping. We selected three samples along the core with high content of lead to identify the type of lead-bearing minerals. For this purpose, samples were previously metallized with carbon using the high vacuum sputter and C-thread coater Leica EM ACE600.

3.2.1.4. XRF analysis for Pb. About 260 samples were already analyzed for Pb by XRF technique in 2010 as part of a master thesis (Chazerand, 2010). For this type of analysis, no external standards, replicates, and blanks were measured, then accuracy, precision and detection limits were not determined. Therefore, this dataset is only used to compare the trend of Pb while the absolute concentrations will not be considered.

3.2.1.5. Total organic carbon. The concentration of total organic carbon (TOC) was calculated from the difference between the concentrations of total carbon (TC) and total inorganic carbon (TIC). TC was analysed with a Carlo Erba 1108 elemental analyser and the measurements were calibrated against an Acetanilide standard (precision generally <0.3 %). TIC was determined by gasometry with calibration to pure calcite, as described by Leone et al. (1988). In this paper, TOC data was used to correlate the AC05 and AL14 cores and to compare trace metal patterns with organic carbon as a possible source, but they will not be discussed from an environmental perspective.

3.2.2. Core AL14

3.2.2.1. XRF core scanning. XRF scanning of core segments AL14 was carried out immediately after core opening using an ITRAX XRF scanner (Cox, Sweden) and 0.2 mm resolution. The core scanner was equipped with a Cr X-ray source and run at 30 kV and 30 mA. Several elemental data (e.g., Ca, K) were used for refining the optical core correlation to produce a composite core succession. Here, we will only show Pb and Ca data (the latter in Fig. S1 of the supplementary material).

3.2.2.2. Total organic carbon. The concentration of TOC was calculated from the difference between TC and TIC, both analysed with a DIMATOC 200 (Dimatec Co. Germany) elemental analyser.

3.3. Data analysis

3.3.1. Censored data

Geochemical datasets often contain censored data (e.g., values below detection limit; <DL). For certain statistical analysis (e.g., regression and cluster) samples or variables with censored data should be removed or replaced using different imputation methods. If censored data account for less than 10 % of the dataset, a "simple substitution" is appropriate (e.g., Palarea-Albaladejo and Martín-Fernández, 2015), such as using a value equal to 65 % of the DL or 65 % of the minimum value for that variable (Martín-Fernández et al., 2003). If censored data exceed 10 %, multivariate methods should be applied (Palarea-Albaladejo and Martín-Fernández, 2015). The censoring pattern in the dataset was analyzed using the CoDapack software v2.03.01 (Comas-Cufi and Thió-Henestrosa, 2011). The result is reported in Fig. S2, and the replaced dataset is shown in Table S4 of the supplementary material.

3.3.2. Downcore data distribution

3.3.2.1. Description. For a preliminary evaluation of downcore data distribution, we calculated summary statistics and detected "peaks". By "peaks", we refer to the highest values within the data distributions, using the median as the threshold. All computations were realized using R 4.2.2 computing environment (R Core Team, 2022). Summary statistics on raw data include minimum, maximum, mean, standard deviation (SD), and 50th percentile (Table 1). Data summaries are also presented in graphical form as boxplots in Fig. S3 of the supplementary material.

3.3.2.2. Geochemical proxies to evaluate factors affecting metal distributions. Several factors can affect the content and the distribution of trace metals in lake sediments (Boyle, 2002). First, the amount of trace metals that reach the aquatic environment depends on the type of sources, the weathering degree, and the transport mechanisms involved. The latter factors affect particle settling rates and grain-size sorting, influencing the distribution of trace metals, which tend to be enriched in fine particles (e.g., Wang et al., 2023). Then, in-lake factors such as diagenetic processes and primary productivity, also play important roles. Diagenetic processes can lead to dissolution and redistribution of elements sensitive to redox conditions, while the production and deposition of calcite and biogenic silica can dilute trace elements concentrations (i.e., the higher the carbonate and silica contents, the lower the concentrations of trace elements). To evaluate these factors, we used different geochemical proxies, starting from in-lake processes.

To evaluate primary productivity, we normalized Ca and Si to Ti, which is solely of detrital origin (Davies et al., 2015). Then, to correct for dilution by carbonate compounds, which are abundant in the sediments of Lake Accesa, we normalized trace elements to the non-carbonate fraction calculated as 100-%$CaCO_3$.

Possible remobilization of trace metals was evaluated using Fe/Mn ratio, being Fe and Mn two elements sensitive to bottom water redox conditions. Indeed, in a reducing environment Fe and Mn become soluble, but Mn is more sensitive. Therefore, an increase in Fe/Mn ratio can indicate more anaerobic bottom water conditions (e.g., Naeher et al., 2013). However, since Fe and Mn can also derive from the catchment, Boyle et al. (2001) suggest comparing Fe/Mn and Fe profiles: if peaks in Fe concentration coincided with peaks in the Fe/Mn ratio, then it is possible that these changes are related to changes in supply from the catchment. On the contrary, they may be related to changes in reducing conditions.

To correct for eventual changes in grain-size, trace elements were normalized to Al, that is commonly used for this purpose, since Al-rich minerals (e.g., phyllosilicates) constitute a significant part of the fine fraction (e.g., Liang et al., 2013).

Moreover, we calculated the trace metals accumulation rate (XAR) using the following formula: $XAR = SAR * GD * [X]$, where [X] is Cu, Zn and Pb concentrations, SAR is the sedimentation accumulation rate and GD is the gamma density as reported by Vannière et al. (2008).

If these factors do not or only marginally affect trace metal distributions along the core, maxima in trace metal distributions should be mainly related to higher input from the catchment and/or sources enriched with trace metals. In order to account for catchment erosion, we normalized trace elements to Ti that can be used as an indicator of allochthonous inputs from the catchment (Davies et al., 2015). Then, to discriminate between possible sources we consider all other analysis performed in this study.

3.3.3. Compositional data (CoDa) analysis

Since compositional data are characterized by constant-sum closures (i.e., single components represent proportion of a whole), they should log-transformed to evaluate reliable and unbiased correlations among variables (e.g., Buccianti and Grunsky, 2014). Thus, the replaced dataset reported in Table S4 was log-transformed using the centered log-ratio

Table 1
Summary statistics of major (wt%) and trace elements (ppm). In the table carbonate content ($CaCO_3$, wt%) and the number of samples below the detection limit for each variable are also reported.

	Al	Si	Ca	Mg	Mn	Na	P	Fe	K	Ti	$CaCO_3$	Li	V	Cr	Ni	Cu	Zn	Ga	Rb	Sr	Y	Zr	Nb	Sb	Cs	Ba	Hf	Ta	La	Ce	Eu	Pb	Th	U
n°<dl	-	-	-	-	1	-	2	-	3	-	2	-	-	-	-	-	-	-	-	-	-	-	-	-	-	-	-	-	-	1	-	-	-
min	0.24	0.64	1.5	0.36	0.001	0.08	0.02	0.1	0.08	0.01	10	2.7	3.7	9	13	4.7	139	0.48	3.9	179	1.1	0.36	0.43	3.5	1.7	26	0.12	0.02	1.2	1.7	0.01	1.4	0.67	1.5
max	11	23	36	1.9	0.43	0.3	0.1	5.6	2.8	0.52	91	132	152	127	77	625	3174	26	199	2462	30	93	18	55	106	619	2.7	1.3	48	91	1.7	1706	14	6.9
mean	4	9.2	22	0.85	0.11	0.15	0.04	2	1.1	0.17	53	42	54	51	39	110	860	9.2	72	1410	8.8	19	4.9	25	39	210	1.1	0.36	15	27	0.53	309	4.5	3.2
median	2.6	6.4	26	0.68	0.07	0.12	0.03	1.2	0.61	0.07	61	33	34	37	36	26	581	5.8	45	1605	5.6	17	2.4	17	28	114	1.1	0.18	7.5	14	0.32	48	2.6	2.9
dev. st.	3.3	6.9	11	0.46	0.12	0.06	0.02	1.8	0.95	0.17	25	33	46	38	19	173	860	8.1	64	599	7.4	20	4.9	17	31	196	0.57	0.36	14	26	0.49	514	3.8	1.5

(*clr*) transformation (Aitchison, 1986), where for the composition $\mathbf{x} = (x_1, x_2, \ldots, x_D)$ with D components or variables, *clr* is defined as:

$$clr(\mathbf{x}) = \left(\log \frac{x_1}{g_m(\mathbf{x})} \quad , \log \frac{x_2}{g_m(\mathbf{x})}, \ldots, \log \frac{x_D}{g_m(\mathbf{x})} \quad \right)$$

where $g_m(\mathbf{x})$ stands for the geometric mean of the row.

To reduce the geochemical dataset to a smaller set of variables and investigate multivariate relationships between them, a compositional *clr*-biplot was generated using the CoDapack software v2.03.01 (Comas-Cufi and Thió-Henestrosa, 2011). In a *clr*-biplot the 2-dimensional space is generated by the two first vectors of an *olr*-basis (*orthonormal log-ratio)* that are respectively represented by the horizontal and vertical axes (ilr.1 and ilr.2) (Gabriel, 1971; Gower and Hand, 1996). A *clr*-biplot show simultaneously the *clr*-variables and the samples. The *clr*-variables are depicted as rays, with their ends called vertex. The ray length indicates variable variability among samples (i.e., the longer the ray, the higher the variability). A segment connecting two vertices is termed a link and its length indicates the variance of the log ratio among the considered variables (as also shown in the variation array). A low variance of the log ratio (i.e., a short link) suggests that the *clr*-variables are proportional, and may carry the same information (e.g., they can be related to the same environmental process). Samples are represented as points; their distribution in the positive or negative part of the ilr axes indicates which are the dominant *clr*-variables. Closely samples have similar compositions. Moreover, samples nearer to the center of the biplot have a composition more representative of the whole population. On the contrary, samples located far away from the center may be potential outliers.

4. Results

4.1. Downcore distribution of major and trace elements

Table 1 shows the summary statistics for major and trace elements (raw data are listed in Table S2 and displayed as boxplots in Fig. S3 of supplementary material). As indicated in Table 1 and the censoring pattern (Fig. S2), values below the detection limit were found for Mn, P, K, $CaCO_3$ and Eu. Since the percentage of censored data for each variable is below 10 % (Fig. S2), a simple substitution was applied using a value equal to 65 % of the minimum for each variable. All elements show great variability in concentrations (Table 1, Fig. S3), with Cu, Zn and Pb reaching maximum values that are two-three orders of magnitude higher than their minimum.

Downcore distributions of all data from core AC05 are reported in Fig. S4 of supplementary material, while selected elements are shown in Fig. 3. These figures show that Ca, $CaCO_3$ and Sr have similar distribution patterns and behave oppositely to other major and trace elements (Fig. S4). Ca and $CaCO_3$ (Fig. 3) exhibit concentrations above the median value below ca. 80 cm (~1000 cal. BP), while above this depth, they show the lowest concentrations detected throughout the core (Fig. 3). All other selected elements (Fig. 3) show their highest values, significantly above the median, in the uppermost part of the core (from 0 to 80 cm) and generally lower values below this depth. In this lower part, Pb and Cu show values above the median at 377.5 cm (~5250 cal. BP), 237 cm (~3585 cal. BP) and 99 cm (~1260 cal BP) while Zn has values slightly higher than the median only at 377.5 cm (~5250 cal. BP) and 216 cm (~3185 cal. BP). The highest concentrations of Al, Si, Fe, Ti, Cu, Zn and Pb occur where darker layers, and thus less calcareous sediments, dominate (Fig. 3). In the upper 80 cm of the core, Cu, Zn and Pb concentrations rise, peaking around 50 cm (~620 cal. BP), before declining toward the top of the core (Fig. 3).

The periodization displayed on the right is divided in two types: that pertaining to European history (on the right), and that commonly used in the West (on the left).On the right: Copper Age from 3500 BCE to 2200 BCE, Bronze Age from 2200 BCE to 700 BCE and Iron Age from 900 to 700 BCE to ~50 BCE according to Pearce (2019), Coles and Harding (1979) and Wells (2011). The Etruscan period started around 800 BCE as noted in a recent publication by Posth et al. (2021) while Western Roman Empire lasted from 27 BCE to 476 CE (e.g., Garnsey et al., 2015). On the left: Neolithic, from 8000 BCE to 3100 BCE; Ancient history, from 3100 BCE to 476 CE; Middle Age, from 476 CE to 1492 CE and Modernity, which can be further divided into Modern times (1492 CE-1789 CE) and Contemporary times (Dizionario di Storia Treccani, available at https://www.treccani.it/enciclopedia/eta-storiche_(Dizionario-di-Storia)/).

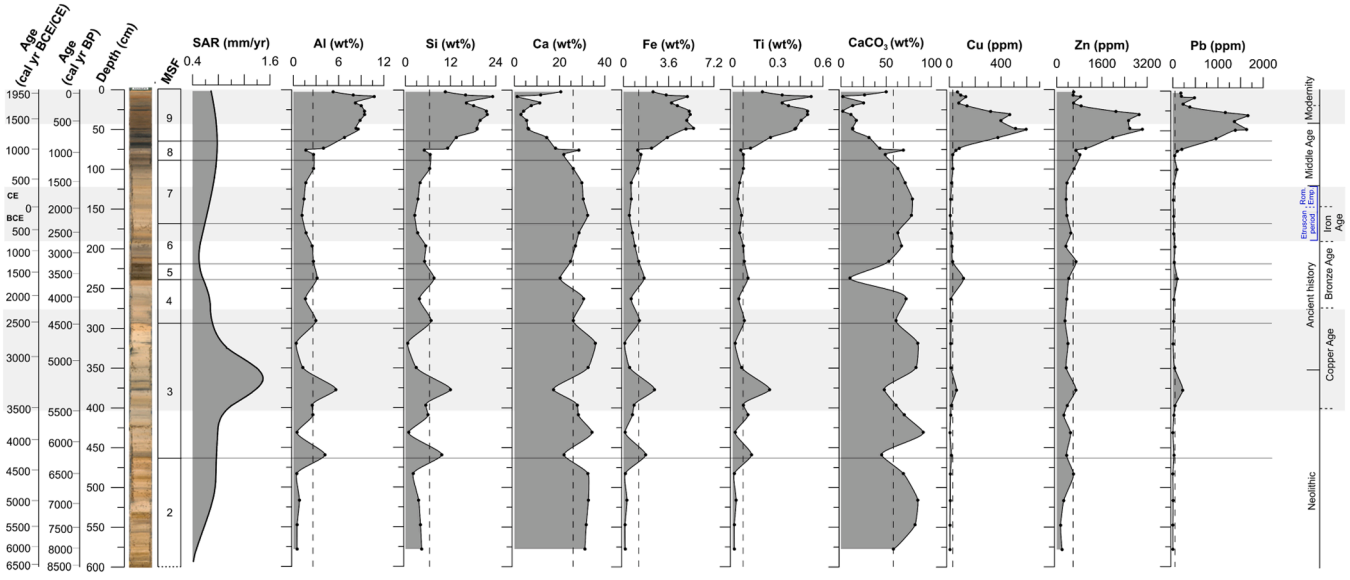

Fig. 3. Plots of selected trace and major elements analyzed in this study on the AC05 core from Lake Accesa. Main sedimentary facies (MSF) and sedimentation accumulation rate (SAR) are from Vannière et al. (2008). MSF1: laminated fine calcareous and organic silty clays; MSF2: laminated calcareous silt; MSF3 and 4: coarsely laminated calcareous clayey silt; MSF5: laminated fine organic silty clays; MSF6: laminated calcareous and organic silty clays; MSF7: coarsely laminated calcareous silt; MSF8: laminated fine calcareous and organic silty clays; and MSF9: laminated fine calcareous clays. Vertical dashed lines indicate median values.

4.2. Multivariate relationships

The compositional statistics summary (geometric center and variation array) is reported in Table S5 of the supplementary material, while Fig. 4 shows the *clr*-biplot of the dataset. The geometric center expressed in % (Table S5) indicates that on average Ca is the most abundant element, followed by Si and Al. Among trace elements, Sr and Zn are on average the most abundant.

The quality of the compositional biplot (Fig. 4A) is quite high, with the first two components (ilr.1 and ilr.2) accounting for about 82 % of the total variance (73 % and 9 %, respectively). The variables with the highest variability (and thus with the longest rays in Fig. 4A) are *clr*-Ca, -Sr, -U, -Pb and -Cu, while *clr*-Al and -Th exhibit the least variability. Based on the low log ratio variance (Tab. S5) and short links in Fig. 4A, proportional variables likely carry similar information are: i) Al, Fe, K, Ti, Ga, Rb, La, Ce and Nb, ii) Na, Mg and P, and iii) Ca, Sr and U. Pb and Cu show high log ratio variance with other variables, while Zn seems quite proportional to Cr, Sb and also Mg and Na. However, Pb has the lowest ratio with Cu, and Cu has the lowest ratio with La.

The compositional biplots (Figs. 4A and B) and the histogram of loadings (Fig. 4C) indicate that almost all elements contribute positively to the first component (ilr.1), except for some mobile elements such as Ca, Sr, U, Mg and Na, and other elements such as Zn, Cr, Sb and Hf. The second component (ilr.2) is instead tied mainly to Cr, Cu, Zn, Pb and Hf, which contribute positively, while other elements contribute negatively. Samples appear to be grouped into three main groups: the largest one is in the lower part of the graph, while the other two groups are distributed in the upper left and right (Fig. 4B). Historical categorization shows that samples on the left are mostly from the Neolithic period, while samples on the right are mostly from the Middle Age and Modern times (Fig. 4B).

4.3. Lead isotopes

Lead isotopes are plotted in Fig. 5 (raw data in Table S3) using a 3D representation based on the $^{206}Pb/^{204}Pb$, $^{207}Pb/^{204}Pb$, and $^{208}Pb/^{204}Pb$ ratios (Fig. 5A), along with biplots based on the $^{208}Pb/^{206}Pb$ and $^{206}Pb/^{207}Pb$ ratios (Figs. 5B and C). Lead isotopes from Lake Accesa are compared with copper ore isotope data from Tuscany, particularly southern Tuscany (Chiarantini et al., 2018; Lattanzi et al., 1997; Stos-Gale et al., 1995), the Island of Elba (Chiarantini et al., 2018) and the Apuane Alps district (Lattanzi et al., 1992), as well as from other Italian areas, including Sardinia (Begemann et al., 2001), the Southeastern Italian Alps (Artioli et al., 2016b) and Liguria (data from the OXALID database). Isotopic signatures for atmospheric lead in Europe related to several anthropogenic sources (e.g., urban, gasoline, industrial) (Bollhöfer and Rosman, 2001; Hansmann and Köppel, 2000) and for the Upper Continental Crust (UCC, Millot et al., 2004) are also included.

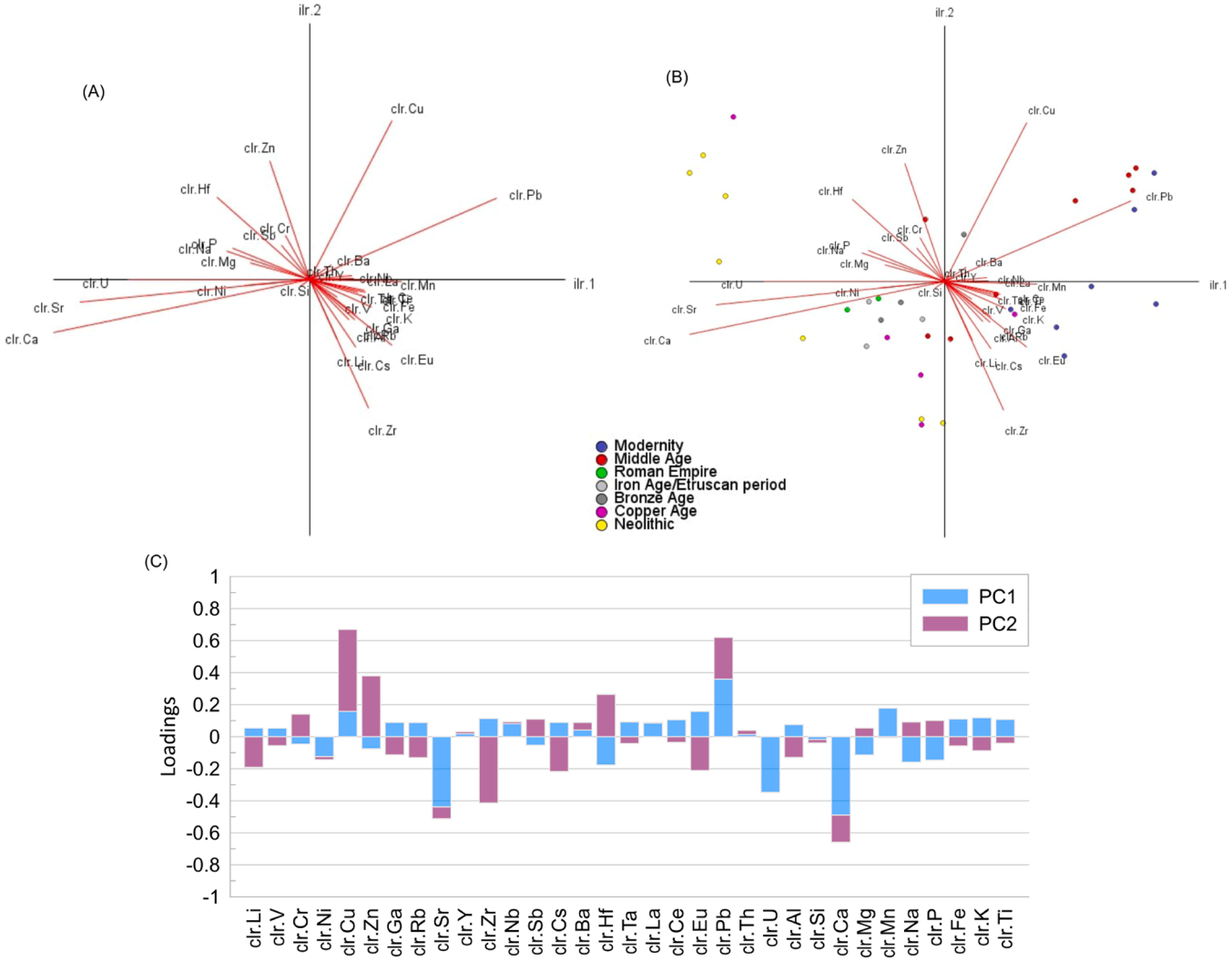

Fig. 4. Compositional *clr*-biplots (α=0.5) A) without sample and B) with samples categorized for the historical period (periodization as described in Fig. 3); C) Stacked histogram of loadings for the first two components (82 % of the total variance).

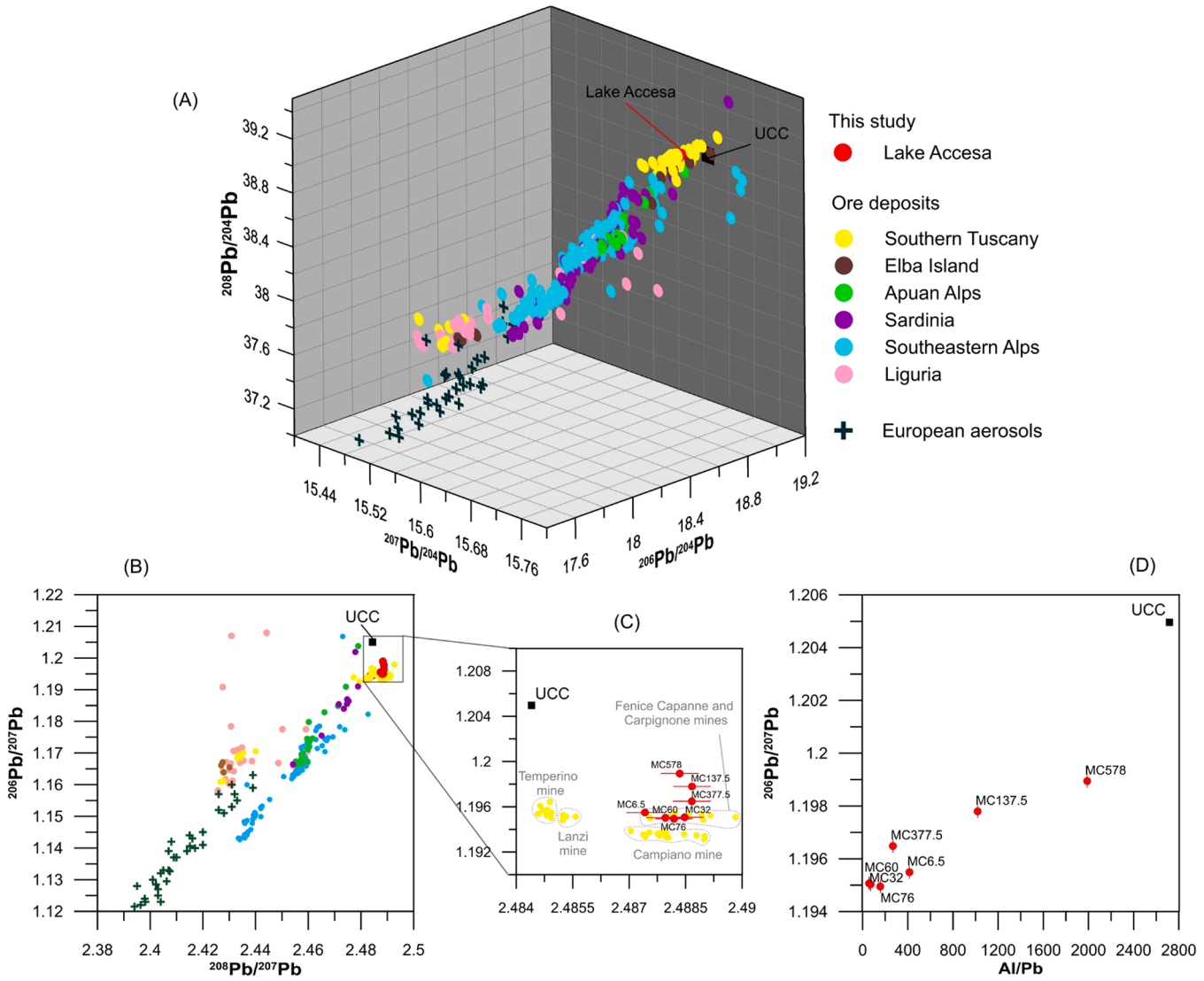

Fig. 5. A) 3D representation based on the $^{206}Pb/^{204}Pb$, $^{207}Pb/^{204}Pb$, and $^{208}Pb/^{204}Pb$ ratios; B) $^{208}Pb/^{206}Pb$ vs. $^{206}Pb/^{207}Pb$ diagram; C) magnified view of diagram (B) for samples from Lake Accesa, highlighting the ore deposits; D) $^{206}Pb/^{207}Pb$ vs. Al/Pb diagram. Lead isotopes from Lake Accesa sediments are compared with copper ores from Southern Tuscany (Chiarantini et al#, 2018; Lattanzi et al#, 1997; Stos-Gale et al#, 1995), the Island of Elba (Chiarantini et al#, 2018), the Apuane Alps district (Lattanzi et al#, 1992), Sardinia (Begemann et al#, 2001), the Southeastern Italian Alps (Artioli et al#, 2016b) and Liguria (data from the OXALID database developed by the Oxford Isotrace Laboratory, http://oxalid.arch.ox.ac.uk/). Isotopic signatures for atmospheric lead in Europe related to several anthropogenic sources (e.g., urban, gasoline, industrial, etc.) (Bollhöfer and Rosman, 2001; Hansmann and Köppel, 2000) and for the Upper Continental Crust (Millot et al#, 2004) are also included. In nearly all graphs, the symbols exceed the size of the analytical error bars.

The lead isotope composition of ore deposits from Southern Tuscany (yellow circles) differs from other copper ores and anthropogenic sources here considered (Fig. 5). Polymetallic ore deposits from southern Tuscany also differ from ophiolitic copper ores which have lower values for all considered ratio. Lead isotopes of Lake Accesa fall within the compositional field outlined by polymetallic ores from southern Tuscany (Figs. 5A and B), particularly those surrounding the catchment area, such as Fenice Capanne and Carpignone mines (Figs. 5 C and 2 A). Notably, samples MC578 and MC137.5 appear distributed between the compositional field of the polymetallic ores and the UCC (Fig. 5C). Fig. 5D highlights the distribution of the samples across two compositional fields.

4.4. FE-SEM analyses

FE-SEM analyses were performed on samples from depths of 32, 60 and 377.5 cm of the AC05 core. For each sample, at least 15 bright minerals, identified with a magnitude of 500x, were examined at higher resolution (Fig. 6A). The most common detected mineral was pyrite (FeS_2) in the framboidal texture (Fig. 6B), which can originate from both biogenic and inorganic processes (e.g., Wilkin and Barnes, 1997). Zircons ($ZrSiO_4$) and monazite $(Ce,La)PO_4$ were also found in all samples. These weather-resistant minerals can accumulate in sediment and soil and be transported to water bodies (e.g., Dill et al., 2012). Grains primarily composed of Sn were recognized as well. Barite ($BaSO_4$) was identified in the samples at 32 and 60 cm of depth. None of the analyzed particles were Pb sulfide minerals (e.g., galena). In all samples, Pb was detected by analyzing areas containing several particles, suggesting that Pb is probably scattered in the bulk sediment. Pb was also found in some grains enriched in Mn in samples at 32 and 60 cm depths.

4.5. Comparison with high resolution XRF data

Pb data from XRF analysis of the cores AC05 and AL14 are shown in Fig. 7 and align closely with the ICP-MS data, showing similar downcore variations. Starting from the bottom, all curves show slight increases

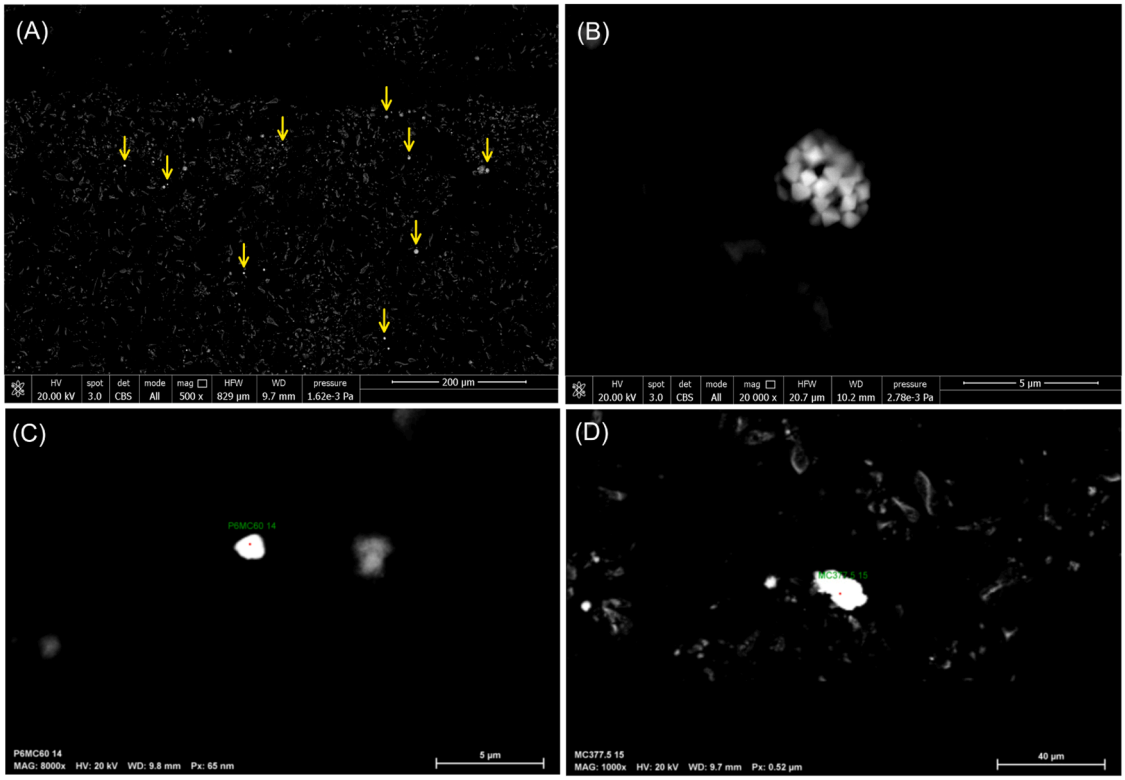

Fig. 6. Backscatter electron images: A) example of bright particles (highlighted by yellow rows) identified with a magnitude of 500x; B) framboidal pyrite; C) monazite; D) grain of tin.

around 5250, 3500 and 1250 cal. BP, while the interspersed periods are characterized by plateaus in Pb contents. The highest Pb contents are observed between 1000 and 250 cal. BP. Additionally, XRF Pb data (Figs. 7C and 7D) show minor increases around 4300 cal. BP and 2750 cal. BP, and a sharp decrease around 700 cal. BP.

5. Discussion

5.1. Variability and sources for trace metals

To interpret trace metal records chronologically, it is important to first evaluate the factors influencing trace metal distributions, as outlined in Section 3.3.2.2, and thus evaluate if the variability of Cu, Zn and Pb patterns is affected by dilution processes linked to lake productivity (Fig. 8A and B), as well as by redox conditions (Fig. 8C) and grain-size sorting (Fig. 8E). The multivariate analysis (Fig. 4) and the pattern of Ca normalized to Ti (Fig. 8A) suggest that Ca is not related to the behavior of Ti but rather it is linked to endogenic calcite precipitation, which is linked to temperature and lake productivity (e.g., Francke et al., 2016). On the contrary, Si appears mostly associated with Ti, suggesting that its main source is detrital input rather than biogenic silica production. The geochemical biplots in Fig. S5 corroborate this interpretation, as *clr*-Ca is negatively related to *clr*-Ti while *clr*-Si exhibits both negative and positive relation with *clr*-Ti, with a predominance of the latter. Consequently, dilution by carbonate compounds may significantly influence trace metals distribution (i.e., the higher the carbonate contents, the lower the concentrations of trace elements). However, since the patterns of trace metals normalized to the non-carbonate fraction (Fig. 8B) closely resemble those of the bulk sediments, the highest concentrations of Cu, Zn and Pb cannot be solely attributed to decreasing carbonate contents. Changing redox conditions appear to have a minimal impact on trace metals distribution as increasing Fe/Mn ratio do not correlate with decreasing trace elements values, and vice versa, especially in the uppermost part of the core (Fig. 8C). Even the patterns of trace metal accumulation rates (Fig. 8D) resemble those of metals concentrations (Fig. 3) indicating that variations in SAR are not the main factor influencing trace metals distributions. Normalization of trace elements to Al (Fig. 8E), as proxy for fine particles, indicates that Zn is likely affected by grain-size sorting, with enrichment in the upper core related to an increase in finer particles. Cu seems only marginally affected in the lowest portion of the core, while Pb shows no variations related to grain-size changes. Similar results are obtained normalizing trace elements to Ti (Fig. 8E), as proxy for catchment erosion. This suggests that the highest Pb values in the core are mainly due to the influx of sources enriched in Pb compared to lithogenic elements such as Ti and Al. In the lower core, Zn appears influenced by sources enriched in this element, becoming proportional to catchment erosion in the upper layers. Cu is probably related to the same sources as Zn from the bottom to about 4500 cal. BP, while from that point to the top of the core, it seems more related to the same sources as Pb.

As regards the type of sources, in the clr-biplot (Fig. 4A), Zn is clustered with elements related to carbonates and organic matter (such as Ca, Sr, Mg, Na and P), while Cu and Pb are positioned separately in the upper right of the graph, suggesting they are triggered by different sources and/or processes compared to the other variables. PC1 likely represents the primary transport and deposition mechanisms in the lake, differentiating between elements transported in solution (on the left) and elements from clastic inputs (on the right). In this case, a possible source for Zn may be thermal water that fed the lake. Then, Zn can precipitate with carbonates and/or be associated with organic matter, being also a nutrient essential for plants (Biester et al., 2012). Consequently, the enrichments in Zn in the basal part of the core (Figs. 8E and 8F) may be related to periods of intense water discharge into the lake. Meanwhile, PC2, mainly tied to Cu, Pb and Zn (Fig. 4), may indicate primary sources enriched in trace metals such as ore deposits and mineralized veins.

Lead isotopes indicate that Pb has a local origin, primarily from polymetallic ores of the Colline Metallifere district, specifically from the

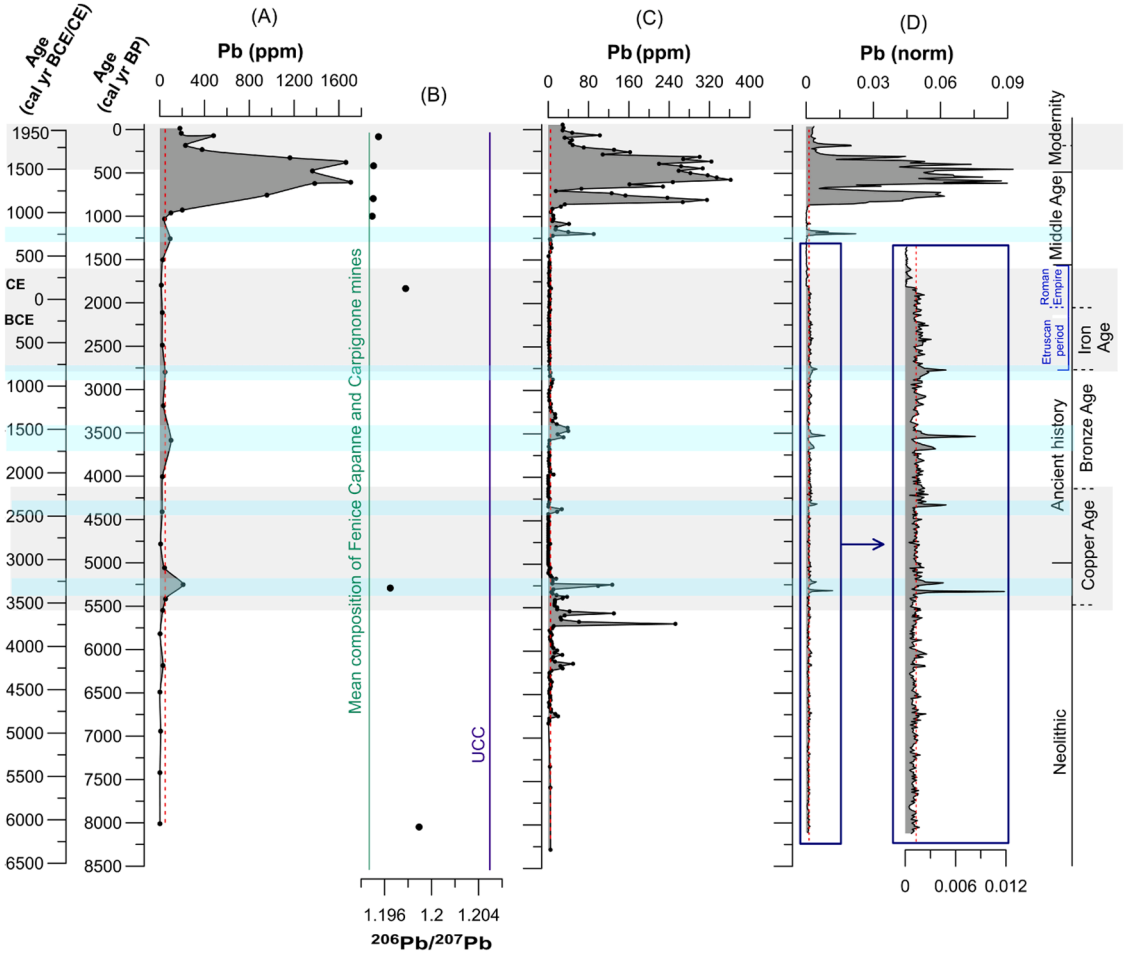

Fig. 7. Pb distributions with depth: A) data from core AC05 obtained via ICP-MS and B) $^{206}Pb/^{207}Pb$ ratio from TIMS analysis. Mean composition of local mines (Stos-Gale et al., 1995) and UCC (Millot et al., 2004) are also reported; C) data from core AC05 obtained via XRF analysis; D) data from core AL14 obtained via XRF core scanning, where Pb (kcps) is normalized by incoherent scatter (kcps) to minimize the effects of organic matter and water content (Davies et al., 2015), resulting in a dimensionless ratio (we reported the calculated mean every 1 cm). Red dotted lines indicate median values for each curve. Prehistoric-historical periodization as described in Fig. 3.

Fenice Capanne and Carpignone mines (Fig. 6C), located near Lake Accesa (Fig. 2). These ores are naturally enriched in Pb, Cu and Zn (Arisi Rota and Vighi, 1971; Burtet-Fabris and Omenetto, 1971), but metal sulfides are nearly insoluble (e.g., Licht, 1988) and can be naturally dispersed mostly through physical erosion. Considering the absence of Pb sulfide minerals in the samples analyzed under the FE-SEM and the high Pb concentrations reached in some samples, it is reasonable to suppose that other mechanisms have enhanced trace metal dispersion from these ores. For example, mining operations produce a large amount of fine and coarse particles, that can disperse through the atmosphere and enter the lake directly or via erosion and runoff from the catchment. During smelting, large quantities of tailings and slags, often rich in residual metals, are also produced. Studies of iron and copper slags from the nearby Massa Marittima district (Fig. 2) showed that Pb, Cu and Zn can reach concentrations up to about 18000, 3000 and 6200 mg/kg, respectively (Rocchi et al., 2023), with varying leachability depending on slags properties and weathering conditions (Rocchi et al., 2022). Today, no slag deposits have been found in the catchment area of Lake Accesa, only in its surroundings. However, it is possible that these slag deposits constituted an important source of metals, especially in the Medieval period.

As stated before, Cu shows a pattern between those of Zn and Pb, suggesting it may be related to multiple sources and processes. However, from around 4500 cal. BP, when Cu's distribution aligns more closely with that of Pb, mining activities likely became the main source of Cu.

Comparison of trace metals with total organic carbon (TOC) reveals no consistent correlation (Fig. 8G), except for the peak detected in the sedimentary facies 5, which also correspond with increases in Cu and Pb (Fig. 8G). Additional potential sources, such as forest fires and volcanic activity, show no clear relationship with trace metals (Fig. 8G) based on comparison with charcoal analysis (Vannière et al., 2008) and major volcanic eruptions in Italy (Zanchetta et al., 2011).

5.2. *Local prehistory and history of lead pollution*

5.2.1. *Neolithic (~6000–3500 BCE)*

Although pollen analyses indicate human presence around Lake Accesa from 8000 cal. BP (Colombaroli et al., 2008; Drescher-Schneider et al., 2007), Pb concentrations remain low and steady until 5500 cal. BP, showing no enrichment compared to Ti (Fig. 8F) and an isotopic composition shifted towards that of the UCC (Figs. 5C and 7B). Therefore, values from this period may reflect the natural background levels for Lake Accesa. Using mean values from this section as reference for calculating enrichment factors (e.g., Barbieri et al., 2015) for Pb, Cu and Zn (Fig. S7 of the supplementary material), produces the same enrichments indicated by Al- and Ti-normalized patterns (Figs. 8E and 8F).

5.2.2. *Copper and Bronze Age (~3500–700 BCE)*

From 5500 cal. BP (~3500 BCE), Pb concentrations start to increase (Fig. 7), reaching a first peak of 208 ppm around 5250 cal. BP (~3300

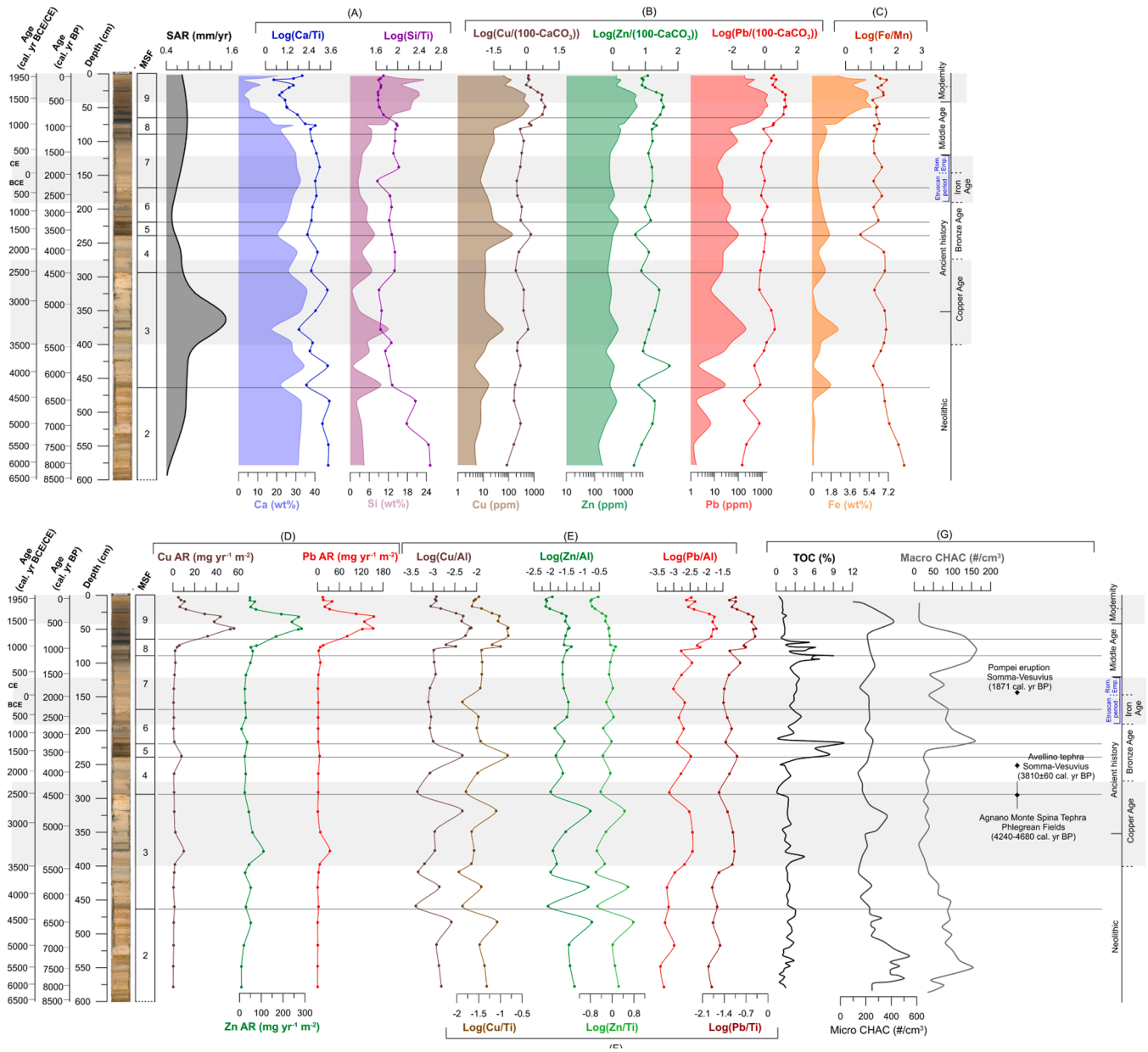

Fig. 8. Evaluation of factors that can affect trace metals distribution: A) lake productivity evaluated by means of Ca/Ti and Si/Ti ratios and the subsequent potential dilution effects by carbonate content (B) evaluated normalizing trace metals to 100-$CaCO_3$. The X-axis of Cu, Zn and Pb are logarithmic; C) redox conditions evaluated by means of Fe/Mn ratio, D) variation in SAR evaluated calculating the trace metals accumulation rate, E) grain-size sorting evaluated normalizing trace metals to Al. Potential sources of trace metals are also evaluated: F) catchment erosion assessed normalizing trace metals to Ti; G) Total Organic Carbon (TOC) analyzed in this study, charcoal concentrations (both micro and macro) as reported by Vannière et al# (2008) and major volcanic eruptions in Italy as reported by Zanchetta et al# (2011). All ratios are reported as logarithms. Prehistoric-historical periodization as described in Fig. 3.

BCE). The Ti-normalized pattern indicates slight Pb enrichment over Ti through most of the Copper Age (Fig. 8F), and isotope analysis of the most concentrated sample shows a composition closer to that of mineralized ores (Figs. 5C and 7B). Presumably this is the first sign of anthropic impact related to mining activities. Although no settlements from this period are confirmed around Lake Accesa (Camporeale and Giuntoli, 2000), human presence and land-use is attested by pollen records (Drescher-Schneider et al., 2007; Vannière et al., 2008). Evidence of early metallurgical activity in southern Tuscany support this interpretation, with the earliest copper-working site (San Carlo mine, near the village of Campiglia Marittima) dated to ~3400–3100 BCE (Artioli et al., 2016a). Notably, two Eneolithic copper axes bear lead isotope signatures typical of the ore districts of southern Tuscany: one from the Iceman Ötzi found in Alto Adige (3300–3100 BCE: Artioli et al., 2017) and another from Zug-Riedmatt, Switzerland (3250–3100 BCE: Gross et al., 2017). The Pb signal detected at Lake Accesa may thus represent the first attempt of exploitation of the deposits around the lake. Additionally, high-resolution Pb data (Fig. 7C) show an increase of Pb around 4300 cal. BP (~2300 BCE) suggesting multiple phases of local ores exploitation during the Copper Age.

The presence of several tin aggregates in the sample at a depth of 377 cm (~5250 cal. BP; ~3520 BCE) may indicate early attempts of tin extraction from cassiterite (SnO_2) for bronze production. While there is no evidence of Sn ore deposits within the Accesa catchment, the presence of Sn mineralization is well-known in the Campiglia Marittima area (e.g., Venerandi-Pirri and Zuffardi, 1982) where Sn was mined both in modern and ancient time, mostly for bronze production (Pampaloni, 2017). This may suggest the transport of tin into the study area for

bronze-making purposes. However, this hypothesis remains speculative and would require corroboration through additional samples from this period and archeological evidence.

Then, Pb levels remain relatively low until 3500 cal. BP (~1550 BCE), when a minor increase appears (Fig. 7C). This period also shows increased fire activity (Vannière et al., 2008) and a shift in environmental conditions, as indicated by a thick organic layer (Fig. 8). Bronze Age copper mining and metallurgy in the area is indicated by the discovery of numerous copper ingots (so called *panelle*) near mining sites, like Serrabottini, close to Lake Accesa. Metal production during this period is further confirmed by the abundance of metal artefacts retrieved in funerary contexts, belonging to the Spilamberto, Massa Marittima and Montemerano types (Aranguren and Sozzi, 2005).

5.2.3. Etruscan period and Roman Empire (~700 BCE – 476 CE)

No significant Pb anomalies are recorded during the Etruscan and Roman periods, aside from a very small pulse detected around 2750 cal. BP (~800 BCE) in the high-resolution pattern of the AL14 core (Fig. 7D). This is unexpected, particularly for the Etruscan period, not only for the tradition of associating major mining activities in this area with this chronological horizon (e.g., Badii, 1931), but especially for the presence of the nearby Etruscan settlement of Macchia al Monte (Fig. 2 A), that lasted from ca. 8th to 6th century BCE (Camporeale, 2017), and whose economy has been linked to ore exploitation. Relying on available data, mining and metallurgical activities in this period were minimal, likely reflected in the minor pulse of the high-resolution patterns (Fig. 7D). Archaeological evidence indicates a metallurgical area within the Etruscan settlement, with furnaces remains (Camporeale, 2002). However, a first archaeometrical assessment on a selection of archaeometallurgical by-products retrieved on the settlement, revealed limited lead and copper smelting residues (Benvenuti et al., 1999), in agreement with our findings, with most samples (pieces of hematite, magnetite, Fe-hydroxides, iron slags) relating to iron metallurgy (Benvenuti et al., 1999). The presence of iron oxides and by-products is notable, as hematite mined on Elba Island was extensively processed in many productive centres along the coast and the first hinterland from the 7th century BCE onward (Corretti and Benvenuti, 2001; Cucini Tizzoni and Tizzoni, 1992), possibly involving Lake Accesa village in this dynamic iron economy.

The absence of lead anomalies during Roman times indicates minimal or no mining/metallurgical activities around the lake. Archaeological evidence indicates that during this period, mining activities persisted in the study area, mainly focused on the exploitation of iron resources, with no current evidence of base metal production in the Colline Metallifere district (Dallai, 2022). Approximately 70 % of the atmospheric Pb found in Greenland ice and released to the environment during Roman times, has been attributed to the mines of Rio Tinto and Murcia in southern Spain (Rosman et al., 1997). Lead isotopes for a sample from this period show a slight shift toward UCC composition (Fig. 7), suggesting that Pb found in Lake Accesa is mainly from the catchment. Thus, even if atmospheric Pb from Spain reached the lake during Roman times, the local signal likely overshadowed it.

5.2.4. Middle ages (476–1492 CE)

Pb concentrations begin to rise around 1250 cal. BP (~700 CE) (Fig. 7), reaching maximum values (~1700 ppm) around 620 cal. BP (~1330 CE). During the Middle Ages, Massa Marittima was a very important mining and metallurgical center, especially for copper and silver production, as testified by archaeological and historical documents (Benvenuti et al., 2014; Chiarantini et al., 2021; Poggi et al., 2023; Rocchi et al., 2023). This period likely saw intense exploitation of ore deposits around Lake Accesa and accordingly, samples from this period show Pb isotope compositions closely matching those of local ores (Figs. 5C and 7). While the role of Massa Marittima as a mining and metallurgical hub is well-known from the 12th century onwards, the Pb peak (Fig. 7) recorded in the 8th century (~1250 cal. BP) is more challenging. After a period of general stagnation during Roman times, archaeology identifies a renewed interest in the exploitation of copper and lead resources from the 8th century, evidenced by the presence of settlements near mining areas, some of which later developed into fortified sites. Archaeological sequences of Cugnano and Rocchette Pannocchieschi castles, both located in Pb- and Ag-rich areas north of Massa Marittima, highlighted the existence of metallurgical and mining structures predating the 10th century (Bianchi, 2022; Rocchi et al., 2023). In addition, isotopic analyses of lead coatings applied to single-fired ceramics (sparse glaze pottery) from the 8th to early 9th centuries, revealed the use of minerals from the Colline Metallifere district (Briano, 2020). The new data from Accesa not only supports previous studies but also, for the first time, highlights early medieval exploitation of copper and lead deposits among the others.

The sharp decrease in Pb concentrations and counts (around tenfold) in high-resolution patterns (Figs. 7C and 7D) at ca. 700 cal. BP (~1250 CE) offers another interesting clue to unveil the economic dynamics related to mine economy in the Middle Ages. During the episcopal control over mining in the Massa Marittima district, which formally ended in 1225 CE with the establishment of the Commune, mining activity was intense, bringing considerable wealth, evident in the architectural flourishing of the city. From the mid-13th century, however, the profitability of mining enterprises began a rapid decline amid significant political upheaval, culminating in the control of the city of Siena over the entire district in 1335 CE. During this time, cadastral sources reveal a progressive decrease in the value of mining company shares, reflecting reduced mine productivity (Pellegrini, 2014). Following the Black Death (bubonic plague) in the late 14th century (about 1350 CE), which decimated a third of the European population (Postan and Miller, 1987), Massa Marittima saw a steep population drop from 5000 to 10000–1500–1600 people (Ginatempo and Sandri, 1990), reducing both labor and demand for metals. However, the recovery seems to have been rather rapid, underscoring the economic importance of mining activities in southern Tuscany.

5.2.5. Modernity (1492 CE – today)

From about 300 cal. BP (~1650 CE), Pb concentrations decrease but remain relatively high (about 300 ppm) compared to lower core sections. During the late 16th century this territory became part of the Grand Duchy of Tuscany and mining activities suffered a decline until the late 1800 CE. In 1900 CE the Montecatini mining company briefly reopened some mines, including Fenice Capanne (Fig. 2), for pyrite extraction, marking the last detectable Pb peak (Fig. 7). All mines in Tuscany were then closed in the 1980s. Accordingly, Pb isotopes from this core section still closely match local ore deposits (Figs. 5C and 7). The decline in Pb levels in this last part of the core may also reflect innovations in mining and refining processes that reduced trace metals dispersion. Over the past 70 years, which are generally characterized by high anthropogenic impacts due to modern activities, Pb levels remain stable (Fig. 7C), but at an average concentration of about 200 ppm (Fig. 7A), suggesting that recent human activity contributed minimal Pb compared to the environmental legacy related to past mining activities in the Lake Accesa area.

5.3. Comparison with other sedimentary archives

In recent decades, several studies worldwide have explored local and regional histories of lead pollution (Cooke et al., 2009; Elbaz-Poulichet et al., 2020; Kamenov et al., 2020; Kern et al., 2021; Kylander et al., 2005; Lee et al., 2008; Longman et al., 2018; McConnell et al., 2018; Pompeani et al., 2013; Renberg et al., 2000). Studies carried out in Greenland ice-cores revealed the hemispheric scope of atmospheric lead pollution especially during Roman and recent times (McConnell et al., 2018 and reference therein, 2019; Rosman et al., 1997). Long-term records from Scandinavia to Central Europe (e.g., Brännvall et al., 1999; Renberg et al., 2000) showed detectable changes in lead pollution

during the Roman (around 2000 years ago), medieval (around 800–1000 years ago) and modern (particularly the 20th century) periods. Similar trends also appear in records from elsewhere, for example France (Elbaz-Poulichet et al., 2011; Sabatier et al., 2020), the Dinaric Alps (Cagliero et al., 2023) and, to a lesser extent, the Swiss-Italian Alps (More et al., 2017). Although the development in Europe has followed the same general course over the last 2000 years, some studies have shown local differences in the history of lead pollution. For example, in some records from Spain (e.g., Corella et al., 2017; Martìnez-Cortizas et al., 1997), the increase in lead during the Roman period is greater than that indicated by records from northern Europe, likely due to the Romans' great reliance on Spanish mines and, therefore, the closer proximity of lead sources. A Serbian record (Longman et al., 2018) uniquely showed lead increase from the Roman period onward, unlike records from Western Europe, where Pb pollution generally declines after the collapse of the Roman Empire, indicating persistent mineral exploitation in the Balkans.

Compared to other selected sedimentary archives in Europe

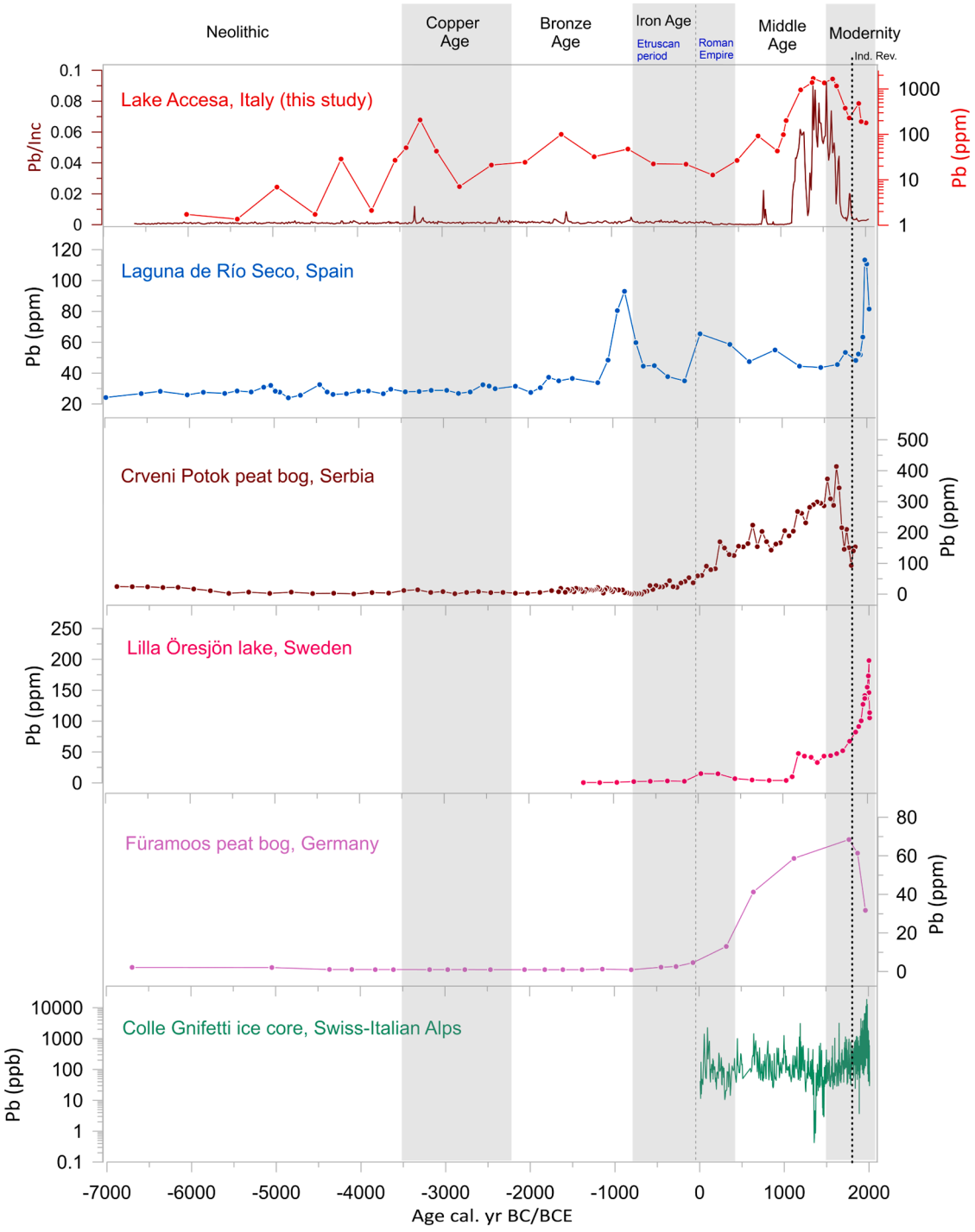

Fig. 9. Comparison of Pb from Lake Accesa (this study) with Pb records from Laguna de Rìo Seco, Spain (García-Alix et al., 2013); Crveni Potok peat bog, Serbia (Longman et al., 2018); Lilla Öresjön lake, Sweden (Renberg et al., 2000); Füramoos peat bog, Germany (Kern et al., 2021); and Colle Gnifetti ice core (More et al., 2017). For Lake Accesa we reported Pb data from ICP-MS on the right (logarithmic scale) and Pb data from XRF core scanning on the left. Historical periodization as described in Fig. 3.

(García-Alix et al., 2013; Kern et al., 2021; Longman et al., 2018; Renberg et al., 2000) and an ice core from Colle Gnifetti in the Swiss-Italian Alps (More et al., 2017), the Lake Accesa record uniquely shows Pb pollution during the Early Copper Age (Fig. 9), indicating a regional phenomenon supported by local archeological evidence. Another study carried out in a mire in northern Spain highlighted the first signal of Pb pollution around 3000 BCE, interpreted as evidence of local mining and metallurgy (Martínez Cortizas et al., 2016). Most archives here reported (Fig. 9) recorded increased Pb levels beginning in the Bronze and/or Iron Age, according to the local and regional history of population growth and expansion of lead metallurgy. All archives document lead pollution during the Middle Age, highlighting that throughout Europe many local Ag-Pb ores were exploited especially for coin production (e.g., Loveluck et al., 2018). Notably, Lake Accesa, which is the closest site to ore deposits among the listed archives, shows the highest Pb levels, not only in the Middle century but also in the Early Medieval period, indicating significant environmental contamination near mining sites. After the Middle Ages, some records (e.g., Laguna de Rìo Seco in Spain and Lilla Öresjön lake in Sweden) show increased Pb concentrations (Fig. 9), correlating with heightened anthropogenic pressure, especially after the Industrial Revolution. In contrast, Lake Accesa shows lower Pb values in the uppermost part of the core compared to the Medieval period (Fig. 9). Interestingly, similar patterns are observed in other records (e.g., Crveni Potok in Serbia and Füramoos in Germany) (Fig. 9). This supra-regional decline is attributed to several factors: i) a period of plagues, famines, and conflict across Europe that decimated the population and brought the economic prosperity of the Late Middle Ages to a halt; ii) the onset of the Little Ice Age, which caused a reduction in crop yields (e.g., Kern et al., 2021); iii) increased exploitation of metal sources in other parts of the world, such as America (e.g., Brännvall et al., 1999), and iv) improvement of technology and regulations in modern times. However, modern pollution levels have not reached pre-industrial contamination levels in these records, indicating that, in some areas, pre-industrial activities left a significant legacy of potential toxic elements in the environment. Notably, all lakes exhibit a general increasing trend in Pb concentrations from the bottom to the top of the cores, regardless of when they reach the maximum values.

6. Conclusions

The multiproxy study of sediment cores from Lake Accesa enabled the reconstruction of the history of trace metals pollution, especially for Pb, over the last 8000 years in this area, constituting Italy's first long continuous record of this kind.

Multivariate analysis and geochemical proxies indicate that Pb distribution was not influenced by authigenic carbonates, grain-size changes, or redox conditions. Instead, Pb variations seem to reflect changes in inputs due to human activity during the Copper Age (~3300 and ~2350 BCE), Bronze Age (~1550 BCE), and a prolonged phase beginning in the Middle Ages (from ~700 CE). Lead isotopes clearly indicate that Pb in Lake Accesa is of local origin and mainly related to local sulfide polymetallic ore deposits. This suggests that Lake Accesa is not affected by distal pollution from other mining sites, or that these signals are completely overshadowed by local signals. Copper distribution mainly aligns with Pb, suggesting that mining was also the primary Cu source starting from 4500 cal. BP, while Zn seems mainly related to in-lake processes (e.g., thermal water that fed the lake and primary productivity) and catchment erosion.

The Pb patterns from Lake Accesa underscore the scope of medieval metallurgical activity across Europe and corroborate the picture derived by archaeological research in southern Tuscany of a renewed interest in the exploitation of copper and lead resources in the early medieval period. This study provides further evidence that mining began around 3300 BCE in the area, consistently with archeological evidence, and confirms minimal exploitation of sulfide deposits during the Etruscan period and no activity in the Roman times, at least in the surroundings of the lake. This case study shows that sedimentary archives near mining areas are crucial for reconstructing the timing and extent of mining and metallurgical activities, especially when combined with archaeological research.

Interestingly, Lake Accesa and other archives show greater pollution during the medieval period than in recent times, indicating that in some areas pre-industrial activities may have left an important legacy of potential toxic elements in the environment, even greater of pollution due to recent activities associated with the Anthropocene (Crutzen et al., 2021). This points out the importance of examining ancient records to identify natural background values of an area, making the determination of these values more challenging.

CRediT authorship contribution statement

Wagner Bernd: Writing – review & editing, Validation, Resources, Methodology, Investigation. **Magny Michel:** Writing – review & editing, Funding acquisition. **Desmet Marc:** Writing – review & editing, Funding acquisition. **Vannière Boris:** Writing – review & editing, Funding acquisition. **Avanzinelli Riccardo:** Writing – review & editing, Validation, Resources, Methodology, Investigation. **Noel Julie:** Writing – review & editing, Validation, Methodology, Investigation. **Caron Benoit:** Writing – review & editing, Validation, Resources, Methodology, Investigation. **Zanchetta Giovanni:** Writing – review & editing, Validation, Supervision, Project administration, Funding acquisition, Conceptualization. **Baneschi Ilaria:** Writing – review & editing, Resources, Investigation. **Bini Monica:** Writing – review & editing. **Fulignati Paolo:** Writing – review & editing, Validation, Investigation. **Dallai Luisa:** Writing – review & editing, Validation. **Pasquetti Francesca:** Writing – original draft, Visualization, Software, Methodology, Investigation, Formal analysis, Data curation, Conceptualization.

Declaration of Competing Interest

The authors declare that they have no known competing financial interests or personal relationships that could have appeared to influence the work reported in this paper.

Acknowledgements

This work is part of the PhD project of Francesca Pasquetti, with a Pegaso - Regione Toscana scholarship. This study was also financially supported by the French CNRS (National Centre for Scientific Research) within the framework of the ECLIPSE program (Past Environment and Climate) and has benefited from the economic support of the Giovanni Zanchetta Fondi di Ateneo.

Appendix A. Supporting information

Supplementary data associated with this article can be found in the online version at doi:10.1016/j.ancene.2025.100464.

Data availability

Data will be made available on request.

References

Aitchison, J., 1986. The statistical analysis of compositional data. In: Cox, N.R., Hinkley, D.V., Rubin, D., Silverman, B.W. (Eds.), Monographs on Statistics and Applied Probability. Chapman & Hall Ltd, London (UK).

Aranguren, B., Sozzi, M., 2005. New data on mining and smelting activities during the Bronze Age in the Massa Marittima Area (Southern Tuscany, Italy). In: Laffineur, R., Driessen, J., Warmenbol, E. (Eds.), Acts of the XIVth UISPP Congress, Section 11. Archaeopress. British Archaeological Reports, Oxford, pp. 197–200.

Arisi Rota, F., Vighi, L., 1971. Le mineralizzazioni a pirite ed a solfuri misti della Toscana meridionale. La Toscan-.-. Merid. Succ. Fusi, Pavia 368–423.

Artioli, G., Angelini, I., Nimis, P., Villa, I.M., 2016b. A lead-isotope database of copper ores from the Southeastern Alps: a tool for the investigation of prehistoric copper metallurgy. J. Archaeol. Sci. 75, 27–39. https://doi.org/10.1016/j.jas.2016.09.005.
Artioli, G., Angelini, I., Addis, A., Canovaro, C., Chiarantini, L., Benvenuti, M., 2016a. Ceramiche tecniche, scorie, minerali e metalli: interpretazione del processo metallurgico., in: Fedeli, L., Galiberti, A. (Eds.), Metalli e Metallurghi Della Preistoria: L'insediamento Eneolitico Di San Carlo-Cava Solvay. Tagete Edizioni, Pontedera, pp. 68–81.
Artioli, G., Angelini, I., Kaufmann, G., Canovaro, C., Dal Sasso, G., Villa, I.M., 2017. Long-distance connections in the Copper Age: new evidence from the Alpine Iceman's copper axe. PLoS One 12. https://doi.org/10.1371/journal.pone.0189561.
Avanzinelli, R., Braschi, E., Marchionni, S., Bindi, L., 2014. Mantle melting in within-plate continental settings: Sr–Nd–Pb and U-series isotope constraints in alkali basalts from the Sicily Channel (Pantelleria and Linosa Islands, Southern Italy). Lithos 188, 113–129. https://doi.org/10.1016/j.lithos.2013.10.008.
Badii, G., 1931. Le antiche miniere del massetano. Stud. Etrusc.-.-. 5, 455–473.
Baker, J., Peate, D., Waight, T., Meyzen, C., 2004. Pb isotopic analysis of standards and samples using a 207Pb–204Pb double spike and thallium to correct for mass bias with a double-focusing MC-ICP-MS. Chem. Geol. 211, 275–303. https://doi.org/10.1016/j.chemgeo.2004.06.030.
Barbieri, M., Nigro, A., Sappa, G., 2015. Soil contamination evaluation by Enrichment Factor (EF) and Geoaccumulation Index (Igeo). Senses Sci. 2, 94–97. https://doi.org/10.14616/sands-2015-3-9497.
Begemann, F., Schmitt-strecker, S., Pernicka, E., Lo Schiavo, F., 2001. Chemical composition and lead isotopy of copper and bronze from nuragic sardinia. Eur. J. Archaeol. 4, 43–85.
Benvenuti, M., Costagliola, P., Chiaverini, J., Mascaro, I., Tanelli, G., Camporeale, G., Giuntoli, S., 1999. An archeometallurgical study at the etruscan settlement of Lago dell'Accesa (southern Tuscany): preliminary results, in: 2eme Congrès International Sur «Science et Technologie Pour La Sauvegarde Du Patrimoine Culturel Dans Le Bassin Méditerranéen» . STAMPA, Paris, pp. 83–83.
Benvenuti, M., Bianchi, G., Bruttini, J., Buonincontri, M.P., Chiarantini, L., Dallai, L., Di Pasquale, G., Donati, A., Grassi, F., Pescini, V., 2014. Studying the Colline Metallifere mining area in Tuscany: an interdisciplinary approach, in: Proceedings of the Research and Preservation of Ancient Mining Areas, Yearbook of the Institute Europa Subterranea, 9th International Symposium on Archaeological Mining History. Trento, pp. 5–8. ⟨https://doi.org/10.13140/2.1.3270.1446⟩.
Bianchi, G., 2022. Archeologia dei beni pubblici. Alle origini della crescita economica in una regione mediterranea (sec. IX-XI). All'Insegna del Giglio, Firenze.
Biester, H., Hermanns, Y.M., Martinez Cortizas, A., 2012. The influence of organic matter decay on the distribution of major and trace elements in ombrotrophic mires - a case study from the Harz Mountains. Geochim Cosmochim. Acta 84, 126–136. https://doi.org/10.1016/j.gca.2012.01.003.
Bindler, R., Renberg, I., Klaminder, J., 2008. Bridging the gap between ancient metal pollution and contemporary biogeochemistry. J. Paleolimnol. 40, 755–770. https://doi.org/10.1007/s10933-008-9208-4.
Blaauw, M., Christen, J.A., Bennett, K.D., Reimer, P.J., 2018. Double the dates and go for Bayes — impacts of model choice, dating density and quality on chronologies. Quat. Sci. Rev. 188, 58–66. https://doi.org/10.1016/j.quascirev.2018.03.032.
Bollhöfer, A., Rosman, K.J.R., 2001. Isotopic source signatures for atmospheric lead: the Northern Hemisphere. Geochim Cosmochim. Acta 65, 1727–1740.
Boyle, J.F., 2002. Inorganic geochemical methods in paleolimnology. In: Last, W.M., Smol, J.P. (Eds.), Tracking Environmental Change Using Lake Sediments. Volume 2: Physical and Geochemical Methods. Klumer Academic Publishers, Dordrecht, pp. 83–141.
Brännvall, M.L., Bindler, R., Renberg, I., Emteryd, O., Bartnicki, J., Billström, K., 1999. The medieval metal industry was the cradle of modern large-scale atmospheric lead pollution in northern Europe. Environ. Sci. Technol. 33, 4391–4395. https://doi.org/10.1021/es990279n.
Briano, A., 2020. La ceramica a vetrina sparsa nella Toscana altomedievale. Produzione, cronologia, distribuzione. All'Insegna del Giglio, Firenze.
Buccianti, A., Grunsky, E., 2014. Compositional data analysis in geochemistry: Are we sure to see what really occurs during natural processes? J. Geochem Explor 141, 1–5. https://doi.org/10.1016/j.gexplo.2014.03.022.
Burtet-Fabris, B., Omenetto, P., 1971. Osservazioni sul giacimento filoniano a solfuri di Zn, Pb e Cu di Fenice Capanne. Rendiconti Società Italiana Mineralogia e Petrologia 27, 393–435.
Cagliero, E., Paradis, L., Marchi, N., Lisztes-Szabó, Z., Braun, M., Hubay, K., Sabatier, P., Čurović, M., Spalevic, V., Motta, R., Lingua, E., Finsinger, W., 2023. The role of fire disturbances, human activities and climate change for long-term forest dynamics in upper-montane forests of the central Dinaric Alps. Holocene 33 (7), 827–841. https://doi.org/10.1177/09596836231163515.
Camporeale, G., 2000. I tipi tombali dell'Accesa (Massa Marittima) dal Villanoviano all'Arcaico, in: Zifferero, A. (Ed.), L'architettura Funeraria a Populonia Tra IX e VI Secolo a.C. All'insegna del Giglio, Firenze.
Camporeale, G., 2002. Sui culti dell'abitato etrusco dell'Accesa (Massa Marittima), in: Rites et Cultes Dans Le Monde Antique. Actes de La Table Ronde Du LIMC à La Villa Kérylos à Beaulieu-Sur-Mer Les 8 & 9 Juin 2001. Académie des Inscriptions et Belles-Lettres, Paris, pp. 21–38.
Camporeale, G., 2017. Sulla genesi della città nell'Italia preromana. Economia, sociologia, urbanistica: il caso dell'insediamento dell'Accesa. Archeologia e Calcolatori 28.2, 69–85.
Camporeale, G., Giuntoli, S., 2000. Il Parco Archeologico dell'Accesa a Massa Marittima. Editrice Leopoldo II, Follonica.
Chazerand, B., 2010. Impact des premières sociétés métallurgiques sur l'environnement méditerranéen. Étude géochimique des séries sédimentaires du Lago di Ledro (Trentino, Italie) et du Lago dell'Accesa (Toscane, Italie). (Master thesis). Université de Franche-Comté, Besancon Cedex.
Chiarantini, L., Benvenuti, M., Costagliola, P., Dini, A., Firmati, M., Guideri, S., Villa, I. M., Corretti, A., 2018. Copper metallurgy in ancient Etruria (southern Tuscany, Italy) at the Bronze-Iron Age transition: a lead isotope provenance study. J. Archaeol. Sci. Rep. 19, 11–23. https://doi.org/10.1016/j.jasrep.2018.02.005.
Chiarantini, L., Benvenuti, M., Bianchi, G., Dallai, L., Volpi, V., Manca, R., 2021. Medieval pb (Cu-ag) smelting in the colline metallifere district (tuscany, italy): slag heterogeneity as a tracer of ore provenance and technological process. Minerals 11, 1–23. https://doi.org/10.3390/min11020097.
Coles, J.M., Harding, A.F., 1979. The Bronze Age in Europe. In: Coles, J.M., Harding, A.F. (Eds.), An Introduction to the Prehistory of Europe c.2000-700 B.C., 1st ed. Routledge, London. https://doi.org/10.4324/9781315748412.
Colombaroli, D., Vannière, B., Emmanuel, C., Magny, M., Tinner, W., 2008. Fire-vegetation interactions during the Mesolithic-Neolithic transition at Lago dell'Accesa, Tuscany, Italy. Holocene 18, 679–692. https://doi.org/10.1177/0959683608091779.
Comas-Cufi, M., Thió-Henestrosa, S., 2011. CoDaPack 2.0: a stand-alone, multi-platform compositional software, in: Egozcue, J.J., Tolosana-Delgado, R., Ortego, M.I. (Eds.), CoDaWork'11: 4th International Workshop on Compositional Data Analysis. Sant Feliu de Guíxols.
Cooke, C.A., Bindler, R., 2015. Lake sediment records of preindustrial metal pollution. In: Blais, J., Rosen, M., Smol, J. (Eds.), Environmental Contaminants, Developments in Paleoenvironmental Research. Springer, Dordrecht, pp. 101–120. https://doi.org/10.1007/978-94-017-9541-8.
Cooke, C.A., Balcom, P.H., Biester, H., Wolfe, A.P., 2009. Over three millennia of mercury pollution in the Peruvian Andes. Proc. Natl. Acad. Sci. 106, 8830–8834. https://doi.org/10.1073/pnas.0900517106.
R. Core Team, 2022. R: A Language and Environment for Statistical Computing.
Corella, J.P., Valero-Garcés, B.L., Wang, F., Martínez-Cortizas, A., Cuevas, C.A., Saiz-Lopez, A., 2017. 700 years reconstruction of mercury and lead atmospheric deposition in the Pyrenees (NE Spain). Atmos. Environ. 155, 97–107. https://doi.org/10.1016/j.atmosenv.2017.02.018.
Corretti, A., Benvenuti, M., 2001. The beginning of iron metallurgy in Tuscany, with special reference to Etruria Mineraria. Mediterranean. Archaeology 14.
Crutzen, P.J., Stoermer, E.F., 2021. The 'Anthropocene' (2000). In: Benner, S., Lax, G., Crutzen, P.J., Pöschl, U., Lelieveld, J., Brauch, H.G. (Eds.), Crutzen and the Anthropocene: A New Epoch in Earth's History. Springer International Publishing, Cham, pp. 19–21. https://doi.org/10.1007/978-3-030-82202-6_2.
Cucini Tizzoni, C., Tizzoni, M., 1992. Le antiche scorie del Golfo di Follonica (Toscana): una proposta di tipologia. Milano: Comune, Ripartizione istituzioni e iniziative culturali, Museo archeologico e Civico gabinetto numismatico, Milano.
Dallai, L., 2014. Massa Marittima nell'età del Codice: una rilettura dei dati archeologici e minerari, in: Farinelli, R., Santinucci, G. (Eds.), I Codici Minerari Nell'Europa Preindustriale: Archeologia e Storia. All'Insegna del Giglio, Firenze, pp. 71–81.
Dallai, L., 2022. Bacini di approvvigionamento e produzione del ferro fra l'Elba e la costa toscana nel Medioevo: recenti acquisizioni e metodologie multidisciplinari per la ricostruzione di un nuovo quadro storico-archeologico. Archeol. Mediev. 49, 95–107.
Davies, S.J., Lamb, H.F., Roberts, S.J., 2015. Micro-XRF Core Scanning in Palaeolimnology: Recent Developments. pp. 189–226. https://doi.org/10.1007/978-94-017-9849-5_7.
Dill, H.G., Weber, B., Klosa, D., 2012. Morphology and mineral chemistry of monazite-zircon-bearing stream sediments of continental placer deposits (SE Germany): ore guide and provenance marker. J. Geochem Explor 112, 322–346. https://doi.org/10.1016/j.gexplo.2011.10.006.
Dini, A., 2003. Ore deposits, industrial minerals and geothermal resources. Period. di Mineral. 72, 41–52.
Drescher-Schneider, R., De Beaulieu, J.L., Magny, M., Walter-Simonnet, A.V., Bossuet, G., Millet, L., Brugiapaglia, E., Drescher, A., 2007. Vegetation history, climate and human impact over the last 15,000 years at Lago dell'Accesa (Tuscany, Central Italy). Veg. Hist. Archaeobot 16, 279–299. https://doi.org/10.1007/s00334-006-0089-z.
Elbaz-Poulichet, F., Guédron, S., Anne-Lise, D., Freydier, R., Perrot, V., Rossi, M., Piot, C., Delpoux, S., Sabatier, P., 2020. A 10,000-year record of trace metal and metalloid (Cu, Hg, Sb, Pb) deposition in a western Alpine lake (Lake Robert, France): deciphering local and regional mining contamination. Quat. Sci. Rev. 228. https://doi.org/10.1016/j.quascirev.2019.106076.
Francke, A., Wagner, B., Just, J., Leicher, N., Gromig, R., Baumgarten, H., Vogel, H., Lacey, J.H., Sadori, L., Wonik, T., Leng, M.J., Zanchetta, G., Sulpizio, R., Giaccio, B., 2016. Sedimentological processes and environmental variability at Lake Ohrid (Macedonia, Albania) between 637ka and the present. Biogeosciences 13, 1179–1196. https://doi.org/10.5194/bg-13-1179-2016.
Francovich, R., Wickham, C.H., 1994. Uno scavo archeologico ed il problema dello sviluppo della signoria territoriale: Rocca San Silvestro e i rapporti di produzione minerari. Archeologia Medievale 21, 7–30..
Gabriel, K.R., 1971. The biplot graphic display of matrices with application to principal component analysis. Biometrika 58, 453–467.
Gallon, C., Tessier, A., Gobeil, C., Alfaro-De La Torre, Ma.C., 2004. Modeling diagenesis of lead in sediments of a Canadian Shield lake. Geochim Cosmochim. Acta 68, 3531–3545. https://doi.org/10.1016/j.gca.2004.02.013.
García-Alix, A., Jimenez-Espejo, F.J., Lozano, J.A., Jiménez-Moreno, G., Martinez-Ruiz, F., García Sanjuán, L., Aranda Jiménez, G., García Alfonso, E., Ruiz-Puertas, G., Anderson, R.S., 2013. Anthropogenic impact and lead pollution throughout the Holocene in Southern Iberia. Sci. Total Environ. 449, 451–460. https://doi.org/10.1016/j.scitotenv.2013.01.081.

2015. Garnsey, P., Saller, R., Elsner, J., Goodman, M., Gordon, R., Woolf, G. (Eds.), 2015. The Roman Empire, 2nd ed. University of California Press, Oakland, California..
Ginatempo, M., Sandri, L., 1990. L'Italia delle città: il popolamento urbano tra Medioevo e Rinascimento (secoli XIII-XVI). Le Lettere, Firenze.
Gower, J.C., Hand, D.J., 1996. Biplots. Chapman & Hall, London.
Gross, E., Schaeren, G., Villa, I.M., 2017. The copper axe blade of Zug-Riedmatt (Canton of Zug, Switzerland) – a key to chronology and metallurgy in the second half of the fourth millennium BC. Arch. Äologische Inf. 40, 213–227.
Hansmann, W., Köppel, V., 2000. Lead-isotopes as tracers of pollutants in soils. Chem. Geol. 171, 123–144. https://doi.org/10.1016/S0009-2541(00)00230-8.
Hawthorne, D., Mitchell, F.J.G., 2016. Identifying past fire regimes throughout the Holocene in Ireland using new and established methods of charcoal analysis. Quat. Sci. Rev. 137, 45–53. https://doi.org/10.1016/j.quascirev.2016.01.027.
Kamenov, G.D., Escobar, J., Elliott Arnold, T., Pardo-Trujillo, A., Gangoiti, G., Hoyos, N., Curtis, J.H., Bird, B.W., Isabel Velez, M., Vallejo, F., Trejos-Tamayo, R., 2020. Appearance of an enigmatic Pb source in South America around 2000 BP: Anthropogenic vs natural origin. Geochim Cosmochim. Acta 276, 122–134. https://doi.org/10.1016/j.gca.2020.02.031.
Kassianidou, V., Knapp, A.B., 2005. Archaeometallurgy in the mediterranean: the social context of mining, technology, and trade. In: The Archaeology of Mediterranean Prehistory. Blackwell Publishing Ltd, pp. 215–251. ⟨https://doi.org/10.1002/9780470773536.ch9⟩.
Kern, O.A., Koutsodendris, A., Süfke, F., Gutjahr, M., Mächtle, B., Pross, J., 2021. Persistent, multi-sourced lead contamination in Central Europe since the Bronze Age recorded in the Füramoos peat bog, Germany. Anthropocene 36. https://doi.org/10.1016/j.ancene.2021.100310.
Kylander, M.E., Weiss, D.J., Martínez Cortízas, A., Spiro, B., Garcia-Sanchez, R., Coles, B. J., 2005. Refining the pre-industrial atmospheric Pb isotope evolution curve in Europe using an 8000 year old peat core from NW Spain. Earth Planet Sci. Lett. 240, 467–485. https://doi.org/10.1016/j.epsl.2005.09.024.
Lattanzi, P., Hansmann, W., Koeppel, V., Costagliola, P., 1992. Source of metals in metamorphic ore-forming processes in the Apuane Alps (NW Tuscany, Italy): constraints by Pb-isotope data. Miner. Pet. 45, 217–229. https://doi.org/10.1007/BF01163113.
Lattanzi, P., Benvenuti, M., Gale, N., Hansmann, W., Koeppel, V., Stos Gale, Z., 1997. Pb-isotope data on ore deposits of Southern Tuscany. Plinius 18, 123–124.
Lee, C.S.L., Qi, S.H., Zhang, G., Luo, C.L., Zhao, L.Y.L., Li, X.D., 2008. Seven thousand years of records on the mining and utilization of metals from lake sediments in central China. Environ. Sci. Technol. 42, 4732–4738. https://doi.org/10.1021/es702990n.
Leone, G., Leoni, L., Sartori, F., 1988. Revisione di un metodo gasometrico per la determinazione di calcite e dolomite. Atti della Soc. à Toscan-.-. di Sci. Nat., Mem., Ser. A 95, 7–20.
Liang, L., Sun, Y., Beets, C.J., Prins, M.A., Wu, F., Vandenberghe, J., 2013. Impacts of grain size sorting and chemical weathering on the geochemistry of Jingyuan loess in the northwestern Chinese Loess Plateau. J. Asian Earth Sci. 69, 177–184. https://doi.org/10.1016/j.jseaes.2012.12.015.
Licht, S., 1988. Aqueous Solubilities, Solubility Products andStandard Oxidation-Reduction Potentials of theMetal Sulfides. Journal of Electrochemical Society 135.
Longman, J., Veres, D., Finsinger, W., Ersek, V., 2018. Exceptionally high levels of lead pollution in the Balkans from the Early Bronze Age to the Industrial Revolution. Proc. Natl. Acad. Sci. USA 115, E5661–E5668. https://doi.org/10.1073/pnas.1721546115.
Loveluck, C.P., McCormick, M., Spaulding, N.E., Clifford, H., Handley, M.J., Hartman, L., Hoffmann, H., Korotkikh, E.V., Kurbatov, A.V., More, A.F., Sneed, S.B., Mayewski, P. A., 2018. Alpine ice-core evidence for the transformation of the European monetary system, AD 640–670. Antiquity 92, 1571–1585. https://doi.org/10.15184/aqy.2018.110.
Martínez Cortizas, A., López-Merino, L., Bindler, R., Mighall, T., Kylander, M.E., 2016. Early atmospheric metal pollution provides evidence for Chalcolithic/Bronze Age mining and metallurgy in Southwestern Europe. Sci. Total Environ. 545–546, 398–406. https://doi.org/10.1016/j.scitotenv.2015.12.078.
Martìnez-Cortizas, A., Pontevedra-Pombal, X., Nòvoa Muñoz, J.C., Garcìa-Rodeja, E., 1997. Four thousand years of atmospheric Pb, Cd, and Zn deposition recorded by the ombrotrophic peat bog of Penido Vello (Northwestern Spain). Water, Air, Soil Pollut. 100, 387–403.
Martín-Fernández, J.A., Barceló-Vidal, C., Pawlowsky-Glahn, V., 2003. Dealing with zeros and missing values in compositional data sets using nonparametric imputation 1. Math. Geol. 35, 253–278.
Mauran, G., Caron, B., Détroit, F., Nankela, A., Bahain, J.-J., Pleurdeau, D., Lebon, M., 2021. Data pretreatment and multivariate analyses for ochre sourcing: Application to Leopard Cave (Erongo, Namibia). J. Archaeol. Sci. Rep. 35. https://doi.org/10.1016/j.jasrep.2020.102757.
Mauran, G., Caron, B., Beck, L., Détroit, F., Noûs, C., Tombret, O., Pleurdeau, D., Bahain, J.J., Lebon, M., 2022. Standardization procedure to provide a unified multi-method elemental compositional dataset, application to ferruginous colouring matters from Namibia. J. Archaeol. Sci. Rep. 43. https://doi.org/10.1016/j.jasrep.2022.103454.
McConnell, J.R., Wilson, A.I., Stohl, A., Arienzo, M.M., Chellman, N.J., Eckhardt, S., Thompson, E.M., Pollard, A.M., Steffensen, J.P., 2018. Lead pollution recorded in Greenland ice indicates European emissions tracked plagues, wars, and imperial expansion during antiquity. Proc. Natl. Acad. Sci. USA 115, 5726–5731. https://doi.org/10.1073/pnas.1721818115.
McConnell, J.R., Chellman, N.J., Wilson, A.I., Stohl, A., Arienzo, M.M., Eckhardt, S., Fritzsche, D., Kipfstuhl, S., Opel, T., Place, P.F., Steffensen, J.P., 2019. Pervasive Arctic lead pollution suggests substantial growth in medieval silver production modulated by plague, climate, and conflict. Proc. Natl. Acad. Sci. USA 116, 14910–14915. https://doi.org/10.1073/pnas.1904515116.
Millot, R., Allègre, C.J., Gaillardet, J., Roy, S., 2004. Lead isotopic systematics of major river sediments: a new estimate of the Pb isotopic composition of the Upper Continental Crust. Chem. Geol. 203, 75–90. https://doi.org/10.1016/j.chemgeo.2003.09.002.
More, A.F., Spaulding, N.E., Bohleber, P., Handley, M.J., Hoffmann, H., Korotkikh, E.V., Kurbatov, A.V., Loveluck, C.P., Sneed, S.B., McCormick, M., Mayewski, P.A., 2017. Next-generation ice core technology reveals true minimum natural levels of lead (Pb) in the atmosphere: Insights from the Black Death. Geohealth 1, 211–219. https://doi.org/10.1002/2017GH000064.
Naeher, S., Gilli, A., North, R.P., Hamann, Y., Schubert, C.J., 2013. Tracing bottom water oxygenation with sedimentary Mn/Fe ratios in Lake Zurich, Switzerland. Chem. Geol. 352, 125–133. https://doi.org/10.1016/j.chemgeo.2013.06.006.
Palarea-Albaladejo, J., Martín-Fernández, J.A., 2015. zCompositions - R package for multivariate imputation of left-censored data under a compositional approach. Chemom. Intell. Lab. Syst. 143, 85–96. https://doi.org/10.1016/j.chemolab.2015.02.019.
Pampaloni, A., 2017. The tin of Campigliese: 40 centuries of usage.
Pearce, M., 2019. The 'Copper Age'—A History of the Concept. J. World Prehist. 32, 229–250. https://doi.org/10.1007/s10963-019-09134-z.
Pellegrini, M., 2014. Prima nota sul frammento d'un catasto di Massa Marittima del primo Trecento. In: Maffei, P., Varanini, G.M. (Eds.), Honos Alit Artes. Studi per Il Settantesimo Compleanno Di Mario Ascheri. Gli Universi Particolari. Città e Territori Dal Medioevo All'età Moderna. Firenze University Press, Firenze, pp. 401–410.
Poggi, G., Dallai, L., Volpi, V., 2023. Mining under the canopy: Unveiling the archaeo-mining record in the Colline Metallifere with LiDAR analysis and multidisciplinary studies. Quat. Int. https://doi.org/10.1016/j.quaint.2023.08.006.
Pompeani, D.P., Abbott, M.B., Steinman, B.A., Bain, D.J., 2013. Lake sediments record prehistoric lead pollution related to early copper production in North America. Environ. Sci. Technol. 47, 5545–5552. https://doi.org/10.1021/es304499c.
Postan, M.M., Miller, E. (Eds.), 1987. The Cambridge Economic History of Europe. Volume II: Trade and Industry in the Middle Ages, 2nd ed. Cambridge University Press, Cambridge.
Posth, C., Zaro, V., Spyrou, M.A., Vai, S., Gnecchi-Ruscone, G.A., Modi, A., Peltzer, A., Mötsch, A., Nägele, K., Vågene, Å.J., Nelson, E.A., Radzevičiūtė, R., Freund, C., Bondioli, L.M., Cappuccini, L., Frenzel, H., Pacciani, E., Boschin, F., Capecchi, G., Martini, I., Moroni, A., Ricci, S., Sperduti, A., Turchetti, M.A., Riga, A., Zavattaro, M., Zifferero, A., Heyne, H.O., Fernández-Domínguez, E., Kroonen, G.J., McCormick, M., Haak, W., Lari, M., Barbujani, G., Bondioli, L., Bos, K.I., Caramelli, D., Krause, J., 2021. The origin and legacy of the Etruscans through a 2000-year archeogenomic time transect. Sci. Adv. 7, 1–16. https://doi.org/10.1126/sciadv.abi7673.
Reimer, P.J., Austin, W.E.N., Bard, E., Bayliss, A., Blackwell, P.G., Bronk Ramsey, C., Butzin, M., Cheng, H., Edwards, R.L., Friedrich, M., Grootes, P.M., Guilderson, T.P., Hajdas, I., Heaton, T.J., Hogg, A.G., Hughen, K.A., Kromer, B., Manning, S.W., Muscheler, R., Palmer, J.G., Pearson, C., van der Plicht, J., Reimer, R.W., Richards, D.A., Scott, E.M., Southon, J.R., Turney, C.S.M., Wacker, L., Adolphi, F., Büntgen, U., Capano, M., Fahrni, S.M., Fogtmann-Schulz, A., Friedrich, R., Köhler, P., Kudsk, S., Miyake, F., Olsen, J., Reinig, F., Sakamoto, M., Sookdeo, A., Talamo, S., 2020. The IntCal20 northern hemisphere radiocarbon age calibration curve (0–55 cal kBP). Radiocarbon 62, 725–757. https://doi.org/10.1017/RDC.2020.41.
Renberg, I., Brännvall, M.L., Bindler, R., Emteryd, O., 2000. Atmospheric lead pollution history during four millennia (2000 BC to 2000 AD) in Sweden. Ambio: A J. Hum. Environ. 29, 150–156. https://doi.org/10.1579/0044-7447-29.3.150.
Rizzotto, M., 1981. Il Lago dell'Accesa (Grosseto) note floristiche e vegetazionali. Atti della societa toscana di scienze naturali. Mem. Ser. B 88, 311–323.
Rocchi, I., Potysz, A., Masotta, M., Rocchi, S., 2022. Experimental weathering of historical slags exposed to rhizosphere-like organic acids and various pH conditions. J. Geochem Explor 243, 107109. https://doi.org/10.1016/j.gexplo.2022.107109.
Rocchi, I., Masotta, M., Rocchi, S., 2023. Petrology of iron and copper slags from historical smelting activity in southern Tuscany. Period. di Mineral. 92, 57–73. https://doi.org/10.13133/2239-1002/17898.
Rosman, K.J.R., Chisholm, W., Hong, S., Candelone, J.P., Boutron, C.F., 1997. Lead from carthaginian and Roman Spanish mines isotopically identified in greenland ice dated from 600 B.C. to 300 A.D. †. Environ. Sci. Technol. 31, 3413–3416.
Sabatier, P., Nicolle, M., Piot, C., Colin, C., Debret, M., Swingedouw, D., Perrette, Y., Bellingery, M.C., Chazeau, B., Develle, A.L., Leblanc, M., Skonieczny, C., Copard, Y., Reyss, J.L., Malet, E., JouffroyBapicot, I., Kelner, M., Poulenard, J., Didier, J., Vannière, B., 2020. Past African dust inputs in the western Mediterranean area controlled by the complex interaction between the Intertropical Convergence Zone, the North Atlantic Oscillation, and total solar irradiance. Climate 16 (1), 283–298. https://doi.org/10.5194/cp-16-283-2020.
Stos-Gale, Z., Gale, N.H., Houghton, J., Speakman, R., 1995. Lead isotope data from the Isotrace Laboratory, Oxford: archaeometry data base 1, Ores from the Western Mediterranean. Archaeometry 37, 407–415. https://doi.org/10.1111/j.1475-4754.1997.tb00802.x.
Stos-Gale, Z.A., Gale, N.H., 2009. Metal provenancing using isotopes and the Oxford archaeological lead isotope database (OXALID). Archaeol. Anthr. Sci. https://doi.org/10.1007/s12520-009-0011-6.
Tanelli, G., 1983. Mineralizzazioni metallifere e minerogenesi della Toscana. Mem. Della Soc. à Geol. Ital. 25, 91–109.
Tassi, F., Bicocchi, G., Cabassi, J., Capecchiacci, F., Vaselli, O., Capezzuoli, E., Brogi, A., 2014. Hydrogeochemical processes controlling water and dissolved gas chemistry at

the Accesa sinkhole (southern Tuscany, central Italy). J. Limnol. 73, 523–535. https://doi.org/10.4081/jlimnol.2014.961.

Vannière, B., Colombaroli, D., Chapron, E., Leroux, A., Tinner, W., Magny, M., 2008. Climate versus human-driven fire regimes in Mediterranean landscapes: the Holocene record of Lago dell'Accesa (Tuscany, Italy). Quat. Sci. Rev. 27, 1181–1196. https://doi.org/10.1016/j.quascirev.2008.02.011.

Venerandi-Pirri, I., Zuffardi, P., 1982. The tin deposit of monte valerio (Tuscany, Italy): pneumatolytic-hydrothermal or sedimentary-remobilization processes? In: Amstutz, G.C., Frenzel, G., Kluth, C., Moh, G., Wauschkuhn, A., Zimmermann, R.A., El Goresy, A. (Eds.), Ore Genesis. Springer, Berlin Heidelberg, Berlin, Heidelberg, pp. 57–65.

Wang, C., Yi, Q., Wan, K., Zhang, J., 2023. Partitioning pattern of metals onto sediment particles in shallow lakes: an exponential decrease with increased particle size and its environmental implications. J. Soils Sediment. 23, 483–495. https://doi.org/10.1007/s11368-022-03389-4.

Weis, D., Kieffer, B., Maerschalk, C., Barling, J., de Jong, J., Williams, G.A., Hanano, D., Pretorius, W., Mattielli, N., Scoates, J.S., Goolaerts, A., Friedman, R.M., Mahoney, J. B., 2006. High-precision isotopic characterization of USGS reference materials by TIMS and MC-ICP-MS. Geochem., Geophys., Geosyst. 7. https://doi.org/10.1029/2006GC001283.

Wells, P.S., 2011. The Iron Age. In: Milisauskas, S. (Ed.), European Prehistory: A Survey. Springer, New York, New York, NY, pp. 405–460. ⟨https://doi.org/10.1007/978-1-4419-6633-9_11⟩.

Wilkin, R.T., Barnes, H.L., 1997. Formation processes of framboidal pyrite. Geochim Cosmochim. Acta 61, 323–339. https://doi.org/10.1016/S0016-7037(96)00320-1.

Zanchetta, G., Sulpizio, R., Roberts, N., Cioni, R., Eastwood, W.J., Siani, G., Caron, B., Paterne, M., Santacroce, R., 2011. Tephrostratigraphy, chronology and climatic events of the Mediterranean basin during the Holocene: an overview. Holocene 21, 33–52. https://doi.org/10.1177/0959683610377531.